Response to Anonymous Referee #1

Thanks a lot for the referee #1's comments. Please kindly find the author's responses (in blue).

Anonymous Referee #1Comments:

The paper is much improved, and all my major points were addressed.

However, for two of the major points still some corrections are suggested, see details below. After these points are addressed, I recommend this paper for publication.

1) Previous major point B:

I still think the possibility of long range transport cannot be completely ruled out (but I agree with the authors that it very probably plays no important role for the observed event). I suggest to change the logic of the discussion about the role of long range transport. In my view the following points are important:

a) In 2015 Spitsbergen is close to the sea ice edge; only in the South of Spitsbergen the sea is free of ice. This means that the sensitivity of satellite observations for the detection of enhanced BrO is high north of Spitsbergen.

b) In the GOME BrO maps enhanced BrO VCDs are observed north and east of Spitsbergen during the period of interest and the days before. However, directly north of Spitsbergen always an area with low BrO VCDs is observed from satellite.

c) Trajectory calculations show that transport from the north takes place. However, it is not very probable that the enhanced BrO over the Kings bay is caused by this long range transport because of the rather low BrO VCDs directly north of Spitsbergen. Also such long range transport would probably have led to a longer period of enhanced BrO.

d) Trajectory calculations show that transport from the east coast of Greenland is not probable. So transport from these areas of enhanced BrO VCDs can very porbably be ruled out.

e) In summary, long range transport as an explanation for the enhanced BrO at Spitsbergen can not be completely ruled out. But given the temporal coincidence of the enhamced BrO and the occurrence of the sea ice at Spitsbergen, it can be concluded that the local production of BrO is the most probable explanation.

In addition I have two suggestions:

-please add trajectory calculations also for 2 days before and 2 days after the event. In this way long range transport patterns could be compared with those on the day of the event.

-In the text you write: 'BrO VCD maps from GOME-2 measurement from 20 April to 13 May are shown in Fig. 10.' But in Fig. 10 measurements start only on April 24. Please make the text and Fig. consistent.

Author's Response:

Thanks for the referee's suggestion. We have improved the discussion part. Please kindly find the change in the revised manuscript part 4.1.

Considering the resolution of the figures, the trajectory calculations for 2 days before and 2 days after the event, as well as the BrO VCD maps from GOME-2 are shown in the appendix part. Only maps from 25th to 28th are shown in the manuscript.

2) Previous major point E:

In Fig. 5 you show DAMFs in the left (top) figure, but SCDs in the right (bottom) figure. Please make both figures consistent. My suggestion would be to simply subtract the 90 ° values from the low elevation values in the right (bottom) figure (then the 90 ° values of the simulated and measured data should both be zero). You might also use the same x-axes for both figures.

Author's Response: Fig. 5 has been revised following referee's suggestions. From the figure, it is more convinced that distribution of BrO is in accordance with model of layer 0-1 km during the enhancement.

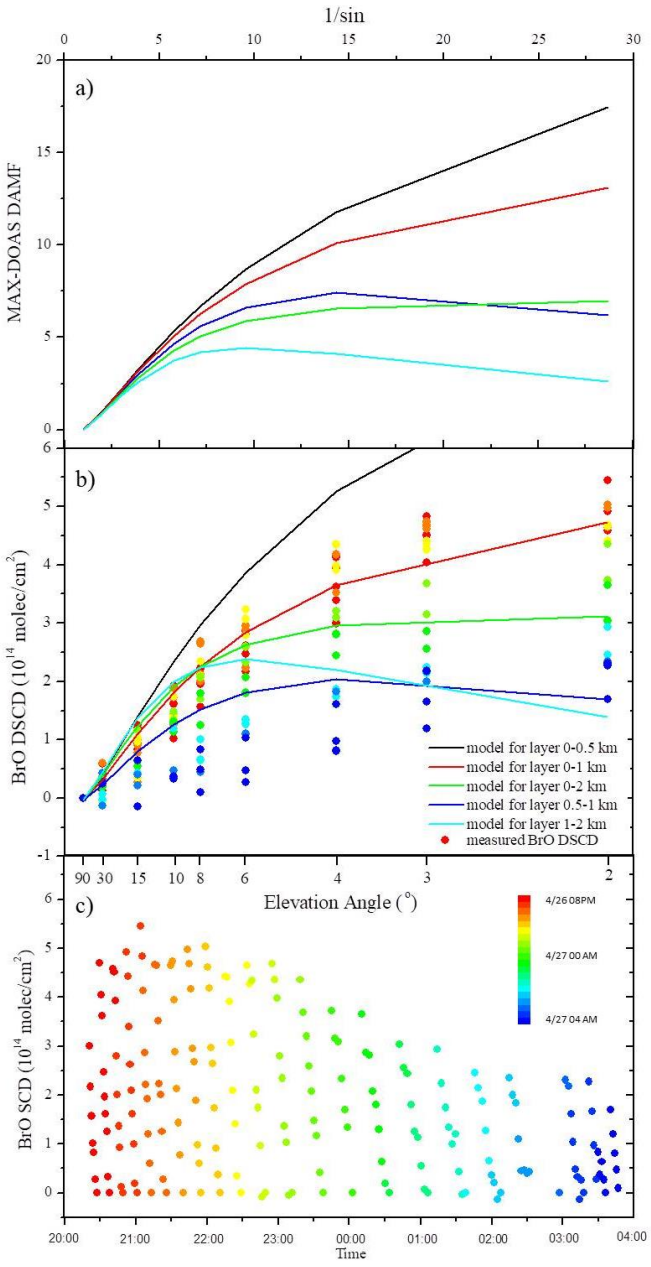

Fig.5 The modeled DAMF (5a) and BrO DSCD (5b) using radiative transfer modeling simulation and the measured BrO DSCDs (5c) from 26/04 20:00 to 27/04 04:00. DAMF are the differences of AMF for low elevation angles and zenith direction. The models are performed assuming a clear sky condition with no aerosol. In part b, the tropospheric BrO VCD is 5×10^{13} molecules/cm^2. The color codes of the measured BrO DSCDs which are also shown in 5b (solid dots) are put into one-to-one correspondence to dots in 5c.

Response to Anonymous Referee #2

It is a pity that the referee #2 has refused the manuscript. We are so sorry that color codes of BrO SCD in Fig.5 might have led to a lot of misunderstandings. Anyway, thanks a lot for the referee #2's comments. And please kindly find the author's responses (in blue).

Anonymous Referee #2 Comments:

The authors put effort into a better interpretation of the MAX-DOAS data concerning the horizontal distribution of BrO. They added the new figure 5 including the results for some radiation transfer calculations and a comparison between observed BrO slant columns as a function of the viewing angle of the instrument and simulated slant columns for different layers of enhanced BRO also as a function of the viewing angle. This corresponds to the additional information requested by both reviewers. Unfortunately, the presentation of these results and the derived conclusions are rather confusing and in my opinion counteract the conclusion of a local ozone depletion event:

1). The authors present the observed BrO slant columns with at least three different color codes, but refer in the title two only two categories (4 hours before or after midnight). Why is that? Why not using only two colors?

Author's Response: We have revised the Fig.5 and added some explanations. The 90 ° values of BrO SCDs are subtracted so that the simulated and measured BrO DSCDs of 90 are all zero. Then we find an even better correlation between modeled BrO DSCDs for layer 0-1km and the measured ones during the enhancement. The color codes refer to the time series of BrO DSCDs from about April 26th 20:00 to April 27th 4:00. The temporal resolution is about two minutes.

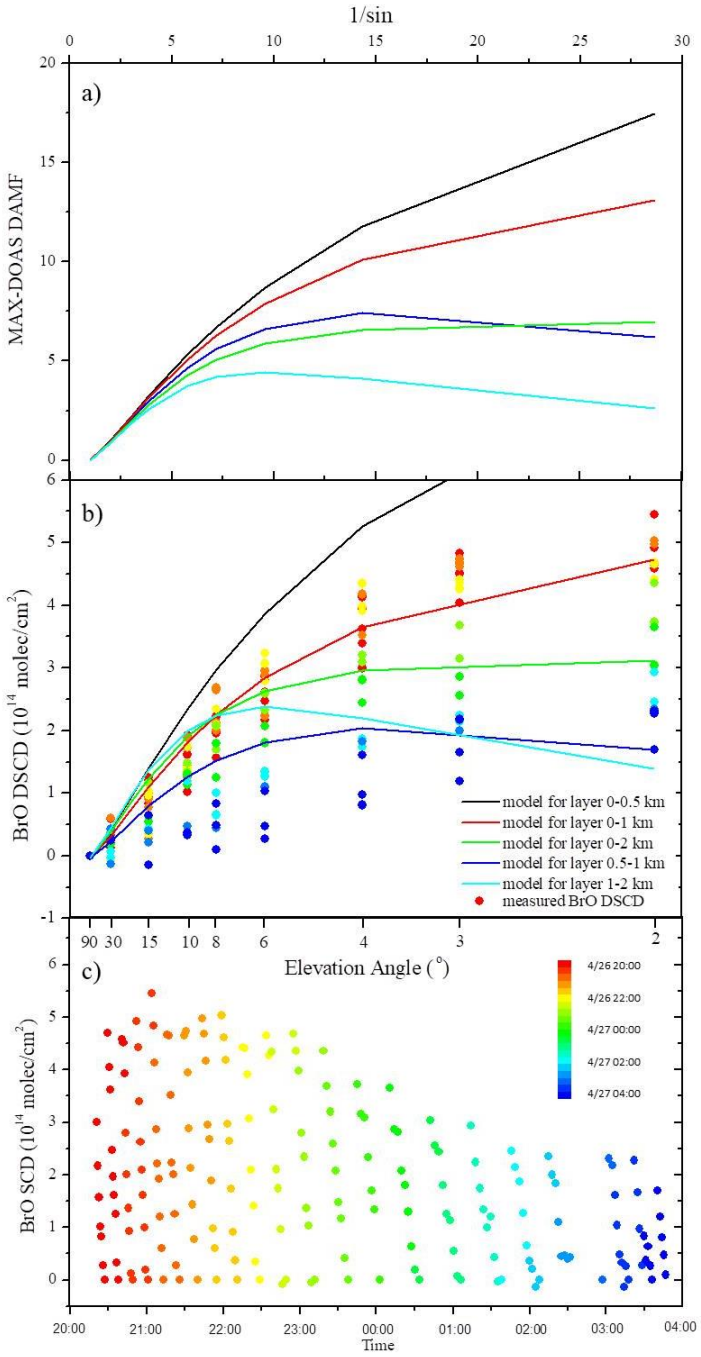

Fig.5 The modeled DAMF (5a) and BrO DSCD (5b) using radiative transfer modeling simulation and the measured BrO DSCDs (5c) from 26/04 20:00 to 27/04 04:00. DAMF are the differences of AMF for low elevation angles and zenith direction. The models are performed assuming a clear sky condition with no aerosol. In part b, the tropospheric BrO VCD is 5×10^{13} molecules/cm^2. The color codes of the measured BrO DSCDs which are also shown in 5b (solid dots) are put into one-to-one correspondence to dots in 5c.

2). What is the reason for using 4-hr averages, although according to figure 13 the entire depletion happened within less than 6 hours with potentially highly variable Br and BrO concentrations?

Author's Response: Highly variable BrO concentrations are shown with temporal resolution of several minutes. No average of BrO DSCD is calculated. Please see Fig. 5 in previous response.

3). With the current figure it is difficult to identify, however, it seems to me that the observations before and after midnight are rather different. Why do the authors then claim that one profile with BrO in the 0-1 km range can explain all observations? Why don't the authors use the highest temporal resolution possible for the observations, which is probably below 30 min for a full scan of all viewing angles?

Author's Response: It is exactly a full scan of all viewing angles with highest temporal resolution of about 2 minutes. From the Fig. 5c, the time series of BrO DSCDs are one-to-one correspondence with Fig. 5b. It is more convinced that distribution of BrO is in accordance with model of layer 0-1 km during the enhancement. Indeed, the 0-1 km range is still a rough estimation of BrO distribution. But it helps to understand the relationship between ozone loss and BrO enhancement in this event.

4). Why do the authors only show results for this specific period? It would be interesting to see the results also for low BrO slant columns.

Author's Response: From Fig.6 and 7, we can find that only within the enhancement event in 26-27 April BrO DSCDs in each elevation angle are differed. While other data is at low level and cannot distinguish between each elevation angle. So it is of less meaning to show the low BrO DSCDs.

5). The authors claim that the observations shown in figure 5 are best reproduced by the BrO profile with a homogeneous layer between 0 and 1 km altitude. Why is that? Fig. 5b actually shows only two simulations with slant columns at 2 ° outside the observed range: BrO in a layer from 0 to 0.5 km and BrO in a layer from 0 to 1 km. The authors do not provide any quantitative information regarding the comparison of the simulations and the results. I find that the best agreement for the period before midnight (blue points) is obtained with the profile with BrO in the layer from 0 to 2 km and for the period after midnight with the profile with BrO in the layer from 0.5 to 1 km. However, this is only based on the visual inspection of the figure. In my opinion, the comparison does not support the claim of the authors that the observed event corresponds to a local BrO formation caused by processes at the surface since

the simulated slant columns for a BrO layer from 0 to 0.5 km are far from all observations at low elevation angles.

Author's Response: The BrO DSCDs are used instead of BrO SCDs in Fig.5 in order to better understand the distribution of BrO by comparing the modelled and measured BrO columns. Please find the new Fig. 5 in previous response. It has to be noted that the inaccuracy of modelled BrO is getting larger at lower elevation angles. So much attention should be paid on the large elevation angles. From Fig.5b, we can see obviously the measured BrO DSCDs before midnight are in good consistence with model for layer 0-1 km.

In summary, the analysis of the presented simulations and observations are to superficial to support the claim of the authors that (1) the simulation with BrO confined to 0 to 1 km corresponds best to the observations and (2) that the BrO increase is a local event. In my opinion, many other scenarios seem equally possible or correspond even better to the presented data.

Regarding the other points raised in my previous report (trajectory analysis, analysis of the mesoscale situation, transport of BrO from the Arctic Ocean, analysis of the boundary layer and impact on the observations, timing of the increase in BrO and decrease of ozone and mercury, sea ice conditions, impact of temperature, significance of calcium carbonate precipitation, measured BrO versus estimated Br) the revised manuscript does not provide a lot of additional information. The authors provide some arguments in the "Author's Response", but most of them are not included in the revised manuscript. Overall, the tone of the manuscript is still the same of the original version, since the authors claim throughout the manuscript that the depletion was a local process without providing a balanced analysis of other possibilities.

Author's Response:

Please find the details in the revised manuscript discussion part.

Response to Anonymous Referee #3

Anonymous Referee #3 General Comments:

Review of Luo et al "Observations and the source investigation of boundary layer BrO in Ny-Aalesund Arctic"

The paper deals with a case of elevated BrO and depleted O3 which the authors state is driven by local processes. The data are interesting, but several statements are contentious, and the conclusions do not sufficiently take into account alternative interpretations. The paper is worthy of publication in ACP, but these fundamental issues must first be dealt with.

Author's Response:

We thank the referee for the positive comments for this study and appreciate for all the valuable comments that have improved this manuscript. Please kindly find the author's responses (in blue).

Major/minor concerns:

1) The authors conclusion is that the event described here is a local event, and that the rate of increasing BrO and of decreasing O3 are really fast. Precisely because they are so unusual, it is extremely important to demonstrate beyond doubt that this is a locally-driven event. At the moment the paper does not do this. There are 3 possibilities that I see:

i) That this event is a result of long-range transport. The event starts at around 17:00 hours on 26 April 2015. This is late in the day, and Global radiation appears to be less than 200W/m2. Trajectory calculations show that the trajectory arriving at 500m agl at noon (the yellow line) travelled at ground level for roughly 2.5 days before rising rapidly to the trajectory end point. The next trajectory had a very different path, reaching the trajectory end point after travelling at roughly 1000m altitude throughout the previous 3 days. i.e. this point in time indicates a discontinuity in air mass origin, and indeed this is reflected in the observational data. The BrO map on 27/4/15 shows an area of enhanced BrO between Svalbard and Greenland, which to me looks as if it is in the path of the trajectory (yellow line) which travelled at the surface. **To help the reader:** Please make the relevant diagrams bigger. I do not see that trajectories arriving at 1000 m asl are relevant, and consider that these could be removed. Also, most of the BrO maps are not needed – the critical ones are 24th to 27th April. Please remove the others and make the ones for 24th to 27th MUCH larger. Then it will be possible to properly compare the trajectories with the BrO maps, and to make sensible assessment of the role of long range transport. If the conclusion is that it's long range transport, we would not need to worry about the low levels of radiation at this time of day.

ii) That this event is driven by the sea ice, but that it is not local to Kings Bay. The coincidence in timing of sea ice arriving in Kings Bay and in the drop in O3 is very interesting. However, the authors' suggestion seems to be that ozone levels are normal until the ice arrives, and then suddenly it drops. My question here is: why should ozone depletion only "switch on" when the

ice arrives in King's Bay..? If the ice is active, wouldn't you expect there to be some sort of equilibrium between the air and the ice, with ozone depletion "travelling with" the sea ice..? Local depletion that has been described before has occurred because the ice has formed locally, or air has traversed an area with new sea ice, which is quite different to this case. If the ice is actively depleting ozone, this could have started before the ice arrived in the Bay, in which case air could already be low in ozone and thus be transported, albeit from a local area of depleted ozone. Here the maps of sea ice are critical, and here there is a bit of a problem. The authors provide the web link to the images, but in none of the files can one find the image that is presented in Fig 11. This inconsistency absolutely has to be explained, and the duration of ice in the Bay demonstrated. If a photo is used, the right and proper citation for the image must be supplied so that readers can look for themselves and assess the local conditions.

iii) That this event is locally-driven. However, it must be explained how depletion could occur at the very low solar radiation levels at this time. The authors state on Page 7, line 21, that the heterogenous reactions can still happen under twilight. However, the catalytic cycle shown in Fig 1 is clearly partly photolytic – please provide evidence that there is sufficient light available for the photolytic parts of the catalytic cycle to proceed at a sufficient rate to explain the observed ozone loss.

Author's Response:

The reviewer discussed three possibilities of this event clearly and deeply in the comment. We appreciate reviewer's hard work and accept many helpful suggestions to improve the manuscript.

We analyze from the following three aspects:

1) The air mass origin

In order to find the detail of the air mass origin, we also calculate the air mass back trajectory in 26th April using HYSPLIT model. It shows air mass at 500 m altitude has different origin before/after 15:00 UTC 26 Apr. The wind direction changed to north with higher velocity. After then, the air mass has a relatively stable origin from 1000 m height.

From the GOME-2 BrO VCD maps, we can find enhanced BrO are observed at east of Greenland (Red box), far north of Siberia (Blue circle) and east of Spitsbergen (Black box) during the period of interest and the days before.

Combining the above information, firstly, trajectory calculations show that transport from the east coast of Greenland and east coast of Spitsbergen are not possible. So transport from these areas of enhanced BrO can be ruled out. Secondly, trajectories also show that after 16:00 UTC 26 Apr transport from the north takes place, which means the high BrO in the blue circle might have influenced this event. However, we have to notice that a). the altitude of air mass is up to 1000 meters; b). there is no enhancement along the path; c). the time scale is unreasonable. The BrO enhancement we found by ground-based MAX-DOAS as well as ozone loss just

lasted for several hours. But the high level of BrO in the blue circle area lasted more than one day. If the high BrO air mass transported from blue circle area, why there is no enhancement along the path?

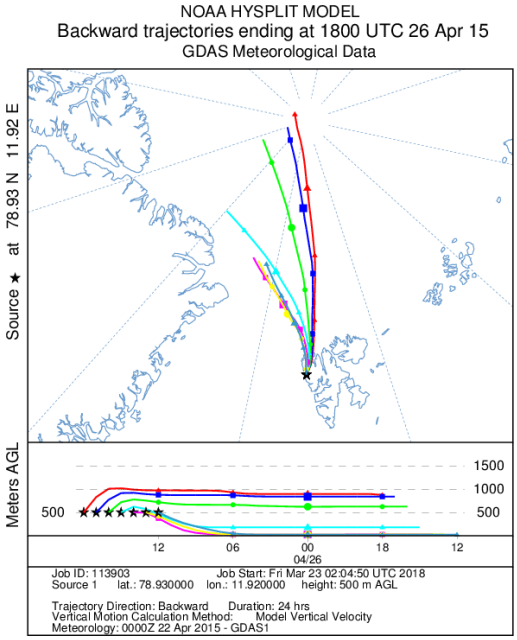

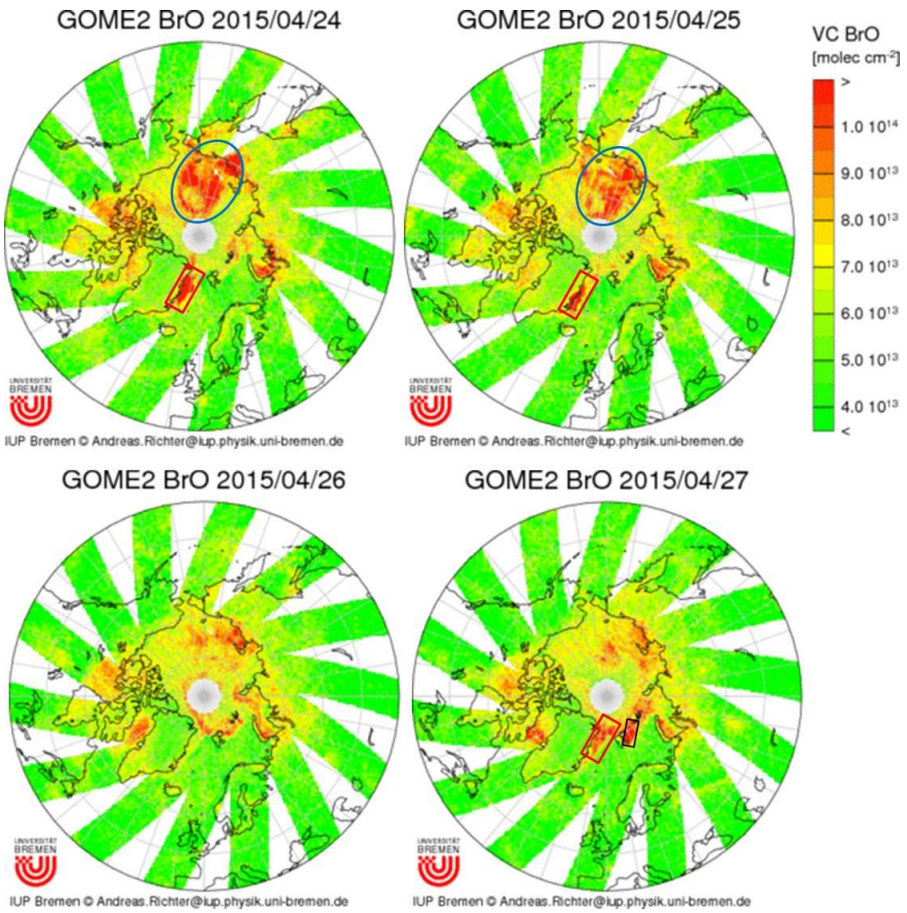

2) The sea ice origin

Firstly, the MODIS remote sensing product and zeppelin webcam have verified

that west of Spitsbergen as well as Kongsfjorden were sea ice free area during April 2015.

Secondly, the sea ice image presented in Fig. 11 is taken by author at 21:00 UTC 26th Apr, which is an unusual phenomenon in the fjord. It is a pity that the zeppelin webcam did not have a clear record of this sea ice process. So we estimated that the sea ice is formed or floated in the fjord after 20:00 UTC 26th Apr.

Now the point is if the sea ice is newly formed or just floated from other area. From the shape of ice in Fig. 11, the sea ice is not looked like newly formed sea ice because of crashed pieces and corrugated edge. So we consider that the sea ice was formed before floating in the bay and transformed to the ice-water mixture when it came across sharply dropped temperature.

3) The ozone depletion

We have changed the time scale to a standard UTC time in each figure, which is very important to analyse this special case of ozone depletion process. In this case, ozone depletion has the anti-correlation with BrO and the ozone loss rate is extremely high compared with previous researches. Taking the ozone loss in Apr 21st, 2015 as an comparison (Figure below), the ozone loss process continued for three days and the ozone loss rate is about 2.5 ug $m^{-3}h^{-1}$. The wind velocity is so high (>10 m/s), and the wind direction is almost unchanged. The air temperature also dropped to very low, which has a good correlation with the ozone concentration. All the evidence showed that the process in Apr 21st is a long-range transport process. But the case in Apr 26th is quite different. The ozone loss rate is much faster while the whole period is quite short instead. The wind velocity is highly variable between 1-7 m/s with unstable wind directions and mixing height.

It is also worth paying attention that the time period that the sea ice existed and the time BrO started to enhance as well as ozone depleted was not exactly the same. From Fig.8 and 12 in the manuscript, the ozone loss started from 14:00 UTC 26th Apr. And as described upon, the sea ice existed in the fjord after 20:00 UTC 26th Apr. It makes the synchronizing variation of BrO and ozone as well as the distribution of 0-1 km reasonable.

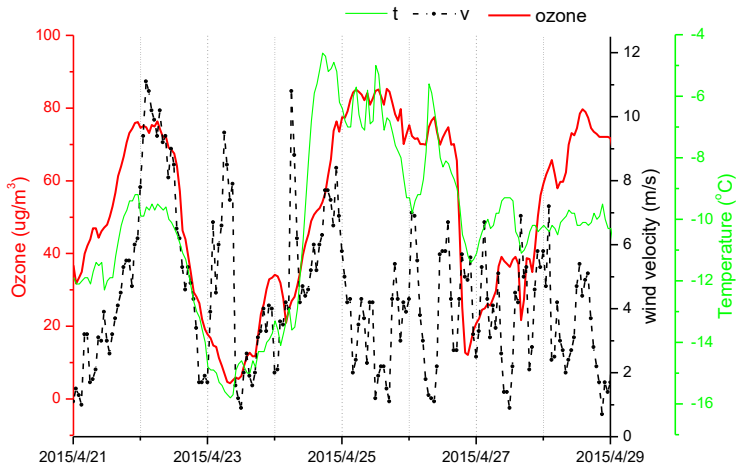

In conclusion, we think the sea ice rather than the long-range transport is the main reason of this event. The sea ice is not totally fresh ice but the low air and water temperature in the fjord might cause the formation of brine ice mixture, which is rich in sea salt aerosols. The sea ice in the fjord is not the trigger of the ozone loss because the ozone loss is occurred earlier than the existence of sea ice.

2) Another major concern is that the location of observations discussed here is not clearly provided. It seems that the MAX-DOAS measuring BrO is located at sea level, and O3 is at 474m on Zeppellin Mountain. Temperature is measured in Ny Alesund. Where is mercury measured? Please state. Also, please show, on Fig 3, the location of Zeppelin Mountain. It seems likely that MAX-DOAS view is over Kings Bay, and that O3, Hg, and temperature are measured in the opposite direction, up on Zeppelin Mountain.

Author's Response:

The locations of the observations are described in part 2.3. MAX-DOAS can measure target trace gases in the troposphere. The analysis of BrO distribution concludes that BrO is located at 0-1km in the troposphere. The BrO results represented the average value of 0-1 km. Ozone and mercury is measured on Zeppelin Mountain, which is at altitude of 480 m a.s.l., representing for the background level of this area. Temperature is from AWI records, which is at ground level. The Zeppelin Station has been marked in Fig.3.

The authors conclude from Fig 5 that the BrO layer 0-1km is the most possible distribution of the BrO. I do not see this so clearly. Please justify this conclusion. Better still, please do the following: Plot Fig 5b as 2 panels, one from 20:00 to 24:00, and one from 00:00 to 04:00 – this will help to clarify where the BrO is, and whether it has moved with time. Also please explain the difference between the red and orange dots? The vertical distribution of BrO is important for the argument of local depletion.

Author's Response:

Fig. 5 has been revised. The 90 ° values of BrO SCDs are subtracted so that the simulated and measured BrO DSCDs of 90 ° are all zero. Then we find an even better correlation between modeled BrO DSCDs for layer 0-1km and the measured ones during the enhancement. The color codes refer to the time series of BrO DSCDs from about April 26th 20:00 to April 27th 4:00. The temporal resolution is about two minutes. It has to be noted that the inaccuracy of modelled BrO is getting larger at lower elevation angles. So much attention should be paid on the large elevation angles. From Fig.5b, we can see obviously the measured BrO DSCDs before midnight are in good consistence with model for layer 0-1 km.

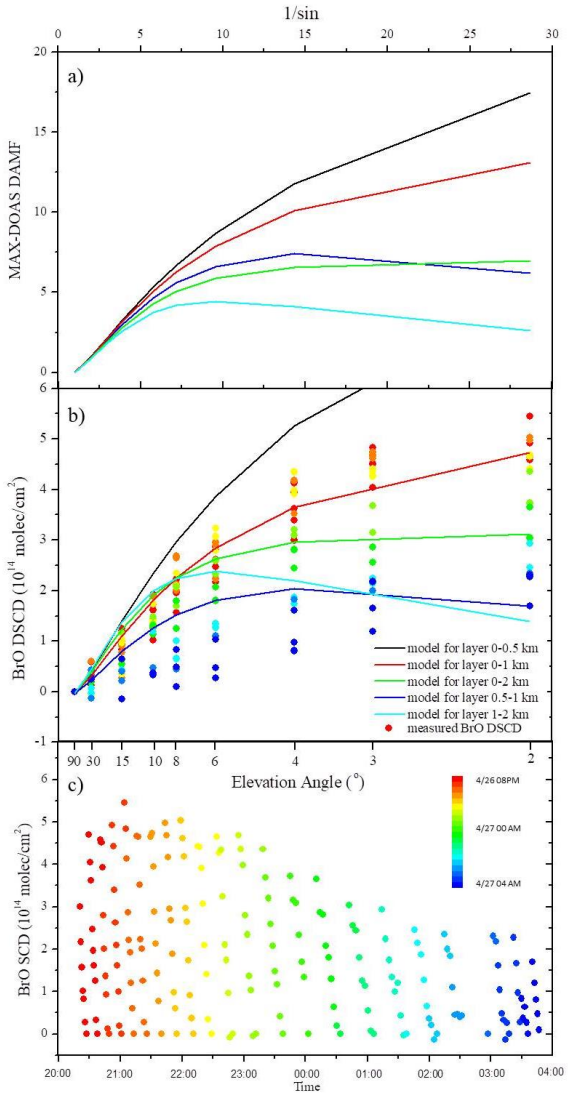

Fig.5 The modeled DAMF (5a) and BrO DSCD (5b) using radiative transfer modeling simulation and the measured BrO DSCDs (5c) from 26/04 20:00 to 27/04 04:00.

DAMF are the differences of AMF for low elevation angles and zenith direction. The models are performed assuming a clear sky condition with no aerosol. In part b, the tropospheric BrO VCD is 5×10^{13} molecules/cm^2. The color codes of the measured BrO DSCDs which are also shown in 5b (solid dots) are put into one-to-one correspondence to dots in 5c.

The authors also state (P5 line 27) that wind velocity during this period is more than 5m/s, but a careful look at Fig 6 shows that the wind velocity is highly variable, ranging between ~7m/s and 1 m/s – it is certainly not simply 5 m/s. This must surely affect air mass movement within the Bay… at low wind speeds, one would not expect much vertical mixing, and if a local process is at play, vertical mixing is essential if the signal of depletion (O3) is measured at 474masl…

Author's Response:

We agree the reviewer's point of view. Especially when compared to the Apr 21st process, which is a typical long-range transport process, this is a regional event occurred at this area.

One minor point, but actually important… If O3 depletion is observed at 474m, there must surely be a lot of sea ice to drive it… I have looked at the web-cam images referred to in the text, and I cannot see evidence of extensive sea ice. Please clarify where the image in Fig 11 came from and provide additional images across this period if possible.

Author's Response:

Please see author's previous response in "2) The sea ice origin". As we know, the area of Kings Bay is about 26 km long and 6 to 14 km wide. At that day, the sea ice floated into the bay and constantly covered the area of the bay. But since no clear webcam evidences, it can just be a reference.

One question, the authors describe that the MAX-DOAS can detect O3… It would help this discussion a lot to show the O3 measured by the MAX-DOAS, even if not very good quality, as it must surely be possible to distinguish between background levels, and none, and this would help with the timing discussion.

Author's Response:

The MAX-DOAS can detect the total column of ozone. But since the stratospheric ozone is far more than tropospheric ozone, it is usually used to calculate stratospheric ozone (the altitude of "ozone layer"). It is difficult to identify the variations of tropospheric ozone by ground-based MAX-DOAS independently.

3) Fig 7. The authors state on Page 6, line 2, that the differences in BrO dSCD <4 degrees is very small – This is hard to assess as red and orange dots are hard to tell apart. To demonstrate this point, please plot only 2, 3, 4, 5, degrees, and use colours that are easy to distinguish.

Author's Response:

We have revised Fig.7. The BrO DSCD of 2, 3, 4 degrees are shown in the upright plot.

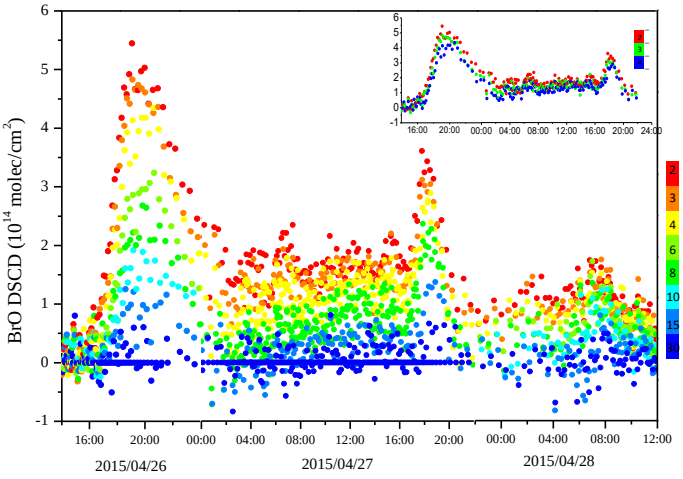

4) Was new sea ice actually forming during this event..? And why did the sea ice dissipate.

Author's Response:

From the shape of ice, it is not looked like newly formed sea ice because of crashed pieces and corrugated edge. But the formation of the ice-water mixture is reasonable because of the low temperature. The saline-ice mixture is also one of the sources of the BrO.

5) Finally, is it possible to learn anything from the fine structure of Fig 8, e.g. the rise in BrO around 22:00 on 27th April..? This, however, must surely be caused by transport given the lack of solar radiation at this time?

Author's Response:

The amount of ozone can be the restriction of the BrO reaction. During the BrO enhancement event, BrO and ozone were maintaining equilibrium between each other. When ozone dropped to the lower limit of the reaction, the reaction of $Br+O_3 \rightarrow BrO+O_2$ would stop (the situation at 26th night). When ozone recovered to a certain level, the reaction restarted. And if there is still enough bromine, ozone will drop again until the reaction is finished. Therefore, the rise of BrO at 22:00 on 27th Apr might be another proves that there is enough sea ice to generate reactive bromine until it melted.

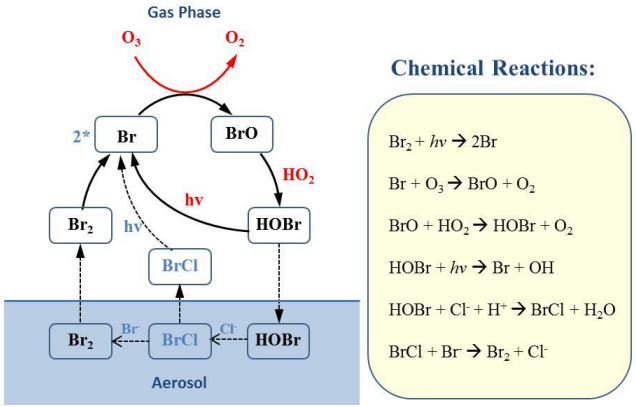

Observations and the source investigations of boundary layer BrO in Ny-Ålesund Arctic

Yuhan Luo[1], Fuqi Si[1], Haijin Zhou[1], Ke Dou[1], Yi Liu[2] and Wenqing Liu[1]

[1] Key Laboratory of Environmental Optics and Technology, Anhui Institute of Optics and Fine Mechanics, ~~Key Laboratory of Environmental Optics and Technology,~~ Chinese Academy of Sciences, Hefei, 230031, China

[2]National Synchrotron Radiation Laboratory, University of Science and Technology of China, Hefei, 230027, China

Correspondence to: Yuhan Luo (yhluo@aiofm.ac.cn) and Fuqi Si (sifuqi@aiofm.ac.cn)

域代码已更改

域代码已更改

Abstract. During polar spring, the presents of reactive bromine in polar boundary layer are considered as the main cause of the ozone depletion and mercury deposition. But many uncertainties still remain in understanding the mechanisms of the chemical process and the source of bromine. As the Arctic sea ice has dramatically reduced recently, it is critical to investigate the mechanism using more accurate measurements with higher temporal and spatial resolution. In this study, a typical process of enhanced bromine and depleted ozone in late April, 2015 in Ny-Ålesund boundary layer was observed applying ground-based Multi Axis-Differential Optical Absorption Spectroscopy (MAX-DOAS) technique. The results showed that there were as high as 5.6 $\times 10^{14}$ molecular cm^{-2} BrO slant columns above the Kings Bay area in 26 April. Meanwhile, the boundary layer ozone and gaseous elemental mercury (GEM) was synchronously reduced by 85% and 90% respectively. Considering meteorology, sea ice distribution and air mass history, the sea ice in the Kings Bay area, emerged only for a very short period time when the enhance BrO was observed, was considered as the major source of this bromine enhancement event. The kinetic calculation showed that the ozone loss rate is 10.3 ppbv h^{-1}, which is extremely high compared to other area. The GEM loss rate is about 0.25 ng m^{-3} h^{-1}. The oxidized GEM may directly deposit to snow/ice and thereby influence the polar ecosystem.

带格式的：默
五号

1 Introduction

Bromine monoxide is one of the key reactive halogen species which have profound impacts on the atmosphere chemistry of the polar boundary layer (PBL), especially the oxidative capacity of the

troposphere (Saiz-Lopez and von Glasow, 2012). The presence of reactive bromine (in some situations "bromine explosion") is considered as the main cause of the depletion of boundary layer ozone, called "ozone depletion events" (ODEs) (Platt and Hönninger, 2003). Furthermore, halogens can efficiently oxidize gas-phase mercury, which can lead to a decrease of gaseous mercury, called "atmospheric mercury depletion events (AMDEs)" (Ariya et al., 2002;Ariya et al., 2004;Lindberg et al., 2002;Lu et al., 2001;Steffen et al., 2008). Enhanced BrO was firstly detected by Long Path Differential Optical Absorption Spectroscopy (LP-DOAS) observations (Platt, 1994). Satellite measurements confirmed that the phenomenon of bromine enhancement covers larger area of polar regions by deriving daily global BrO map (Richter et al., 1998);(Platt and Wagner, 1998;Wagner et al., 2001;Sihler et al., 2013).-The primary source of reactive bromine has been explained by a series of photochemical and heterogeneous reactions at the surface of~~occurred over the~~ frozen ocean during polar spring (Fan and Jacob, 1992). A typical heterogeneous reaction model between gaseous and condensed phases was shown in Fig.1. Bromine is released from salty ice surfaces to the atmosphere in an autocatalytic chemical mechanism that oxidizes bromide to reactive bromine. The reaction of HOBr in aerosol is proposed to be the pivot to explain the recycling reaction, which is an acid-catalyzed reaction (Simpson et al., 2007). Sea-ice (first year) surfaces, brine, and frost flowers have been considered as possible source of bromide aerosols (Kaleschke et al., 2004) (Lehrer et al., 2004).

However, the true circumstance is that the ODEs and BrO enhancement are not always in consistency. There are only few reports of Arctic ODEs that are assumed to have been observed primarily as a result of local-scale chemical mechanism (Bottenheim et al., 2009;Jacobi et al., 2006). As the photochemical reactions are quickly happened and the lifetime of the intermediate products, e.g. the reactive bromine radicals are quite short, more accurate data with higher temporal resolution are needed to analyzing chemical process in PBL and investigating source of bromine.

MAX-DOAS (Multi-AXis Differential Optical Absorption Spectrometer) technique has the advantage of being able to separate clearly the tropospheric and stratospheric portions of the atmospheric column, and even derive a crude vertical profile (Frieß et al., 2011). When pointing to a direction slightly above the horizon, high sensitivities for the trace gases close to the ground can be obtained due to the long light path through the trace gas layers. It is also an important

域代码已更改
域代码已更改
域代码已更改
域代码已更改
域代码已更改
域代码已更改
域代码已更改
域代码已更改
域代码已更改

calibration of satellite observations, which has lower spatial and temporal resolution compared with ground-based measurements. In the Arctic area, ground-based MAX-DOAS observations have been made at Barrow, Alaska (71 °N, 157 °W), Alert, northern Canada (82.5 °N, 62.3 °W) and Ny-Ålesund, Svalbard (78.9°N, 11.8°E) (Tab.1). Besides, air-borne (Neuman et al., 2010;Pöhler et al., 2013) and ship-borne measurements (Bottenheim et al., 2009;Jacobi et al., 2006;Leser et al., 2003;Wagner et al., 2007) are important supplements for the analysis and modelling of bromine chemistry.

However, recently the Arctic sea ice coverage has dramatically reduced, especially at East Greenland and North of Europe. Influenced by the North Atlantic Warm Current (NAWC), the near surface air temperature and sea surface temperature (SST) are getting higher at North Europe (Fig.2). In recent years, Kings Bay in Ny-Ålesund has ice-free open water all year round, which is a unique character comparing with other parts at the same latitude in Arctic. Therefore, it is critical to have a better understanding of the possible reactive bromine source and the impact of the halogen activation on PBL ozone depletion and mercury deposition under a rapidly change Arctic.

In this study, we have caught a unique process of enhanced bromine and depleted ozone in Ny-Ålesund in late April. The key role of bromine was confirmed by ground-based MAX-DOAS measurements. This event provides a rare opportunity to investigate the source of bromine and process of ozone depletion at this area. Kinetic studies of ozone depletion and gaseous mercury deposition are discussed afterwards.

2 Instruments and methods

2.1 Instrument setup

The MAX-DOAS measurement site is located at Yellow River Station (78°55′30”N, 11°55′20”E) at Ny-Ålesund, west coast of Spitsbergen. The observation position is shown in Fig. 3. To have a rough idea of the climate condition, monthly mean sea ice concentrations anomalies and air temperature anomalies in April 2015 are demonstrated in Fig. 2. The observations were carried out from 25 April to 15 May 2015. Due to the wavelength adjustment, no data is available during a short period from 28 to 29 April.

带格式的：默
五号，字体颜
域代码已更改
带格式的：字
New Roman
域代码已更改

The MAX-DOAS instrument operated at Ny-Ålesund consists of indoor and outdoor parts. The telescope receiving scattered sunlight from multi angles is controlled by a stepper motor to adjust elevation angles from horizon (0 °) to zenith (90 °). The field of view of the telescope is about 1 °. The scattered sun light is imported through the quartz fiber with numerical aperture of 0.22 into the indoor spectrograph (Ocean Optics MAYA pro) with a one dimensional CCD (ILX511 linear array CCD) containing 2068 pixels. The wavelength range of the spectrograph is from 290 nm to 420 nm, thus enabling the analysis of trace gases including O_3, NO_2, BrO, OClO, HCHO, and O_4. The spectral resolution is about 0.5nm (FWHM). The CCD detector is cooled at -30 ℃ while the whole spectrometer is thermally stabilized at +20 ℃ using a thermal controller. A computer sets the configuration of the system and controls the automatic measurements. The integration time (typically from 100 ms to 2000 ms multiple 100 scan times) of each measurement depends on the intensity of scattered light which can be influenced by cloud and visibility. The standard mercury lamp is used for spectra calibration. Calibration measurements of dark current and offset are performed after each measurement.

The telescope is pointed towards Northeast direction, which covers the Kings Bay area (Fig.3). Kings Bay is an inlet on the west coast of Spitsbergen, one part of the Svalbard archipelago in the Arctic Ocean. The inlet is 26 km long and 6 to 14 km wide. The range of MAX-DOAS measurement is about 10km radius area, which covers the central area of the fjord. The sequence of elevation angles is 2 °, 3 °, 4 °~~, 5 °~~, 6 °, 8 °, 10 °, 15 °, 30 °and 90 °above the horizon.

2.2 Data evaluation

The spectra measured with the above described setup are analyzed using the well-established DOAS retrieving method (Platt, 1994). The wavelength calibration was performed using the QDOAS software developed by the Belgian Institute for Space Aeronomy (BIRA) by fitting the reference spectrum to a high resolution Fraunhofer spectrum (Kurucz et al., 1988). The spectral analysis of BrO is performed at 340-359 nm, encompassing three BrO absorptions bands, which improves the accuracy of the inversion. O_3 (223K, 243K) (Bogumil et al., 2003;Vandaele et al., 1998), NO_2 (298K, 220K) (Vandaele et al., 1998), O_4 (Hermans et al., 2003), BrO (228K) (Wilmouth et al., 1999), OClO (233K) (Kromminga et al., 2003), and Ring Structure (Chance and

域代码已更改
域代码已更改
带格式的：字
自动设置
域代码已更改
域代码已更改
域代码已更改
域代码已更改
域代码已更改
域代码已更改
域代码已更改

Spurr, 1997) are involved in the inversion algorithm. The O_4 retrieval is performed using the same set of cross sections as for BrO but in the wavelength interval at 340-370 nm. The high resolution cross sections were convoluted with the instrument slit function determined by measuring the emission line of a mercury lamp. A fifth order of polynomial was applied to eliminate the broad band structures in the spectra caused by Rayleigh and Mie scattering. Furthermore, a nonlinear intensity offset was included in the fit to account for possible instrumental stray light. A wavelength shift and stretch of the spectra was allowed in the fit in order to compensate for small changes in the spectral adjustment of the spectrograph.

The fit procedure yields differential slant column densities (dSCD) using noon time zenith sky measurements as Fraunhofer reference for the analysis. An example of the fit result of BrO ~~and O_4~~ is shown in Fig.4. The spectrum was recorded on 26 April, 2015 19:59 UTC (SZA=86°) at the elevation angle of 2°. The BrO dSCD is 5.10×10^{14} molecular cm^{-2}. The residual root mean square is 4.59×10^{-4}, resulting in a statistical BrO dSCD error of 1.63×10^{13} molecular cm^{-2}. The DSCDs of BrO at elevation angle 2° were obtained by subtracting 90°of each sequence, which eliminate the influence of stratosphere BrO change.

Since DSCDs are dependent on the light path, wavelength and observation geometry, DSCDs are then converted to vertical column density ~~(VCD)~~ by dividing the differential air mass factor (DAMF), which is the averaged light path enhancement for solar light traveling through the atmosphere compared to a straight vertical path.

We perform the radiative transfer modeling (RTM) simulations using SCIATRAN (Rozanov et al., 2005) to get modeled DAMF using five different assumed BrO profiles with evenly distributed air masses: a. 0-0.5 km; b. 0-1 km; c. 0-2 km; d. 0.5-1 km; e. 1-2 km (Fig.5a). The models are performed under clear sky condition with no aerosol input. Remarkable difference exists for different input profiles. For BrO layer 0-0.5km, 0-1 km and 0-2 km, DAMFs all increase with the decrease of elevation angles. While for BrO layer 0.5-1 km and 1-2 km, the dependence on the telescope elevation angle is weaker especially at small elevation angles.

The modeled BrO DSCDs for different input BrO profiles are shown in Fig.5b. The input BrO VCD is 5×10^{13} molecules/cm^2. The measured BrO DSCDs from 20:00 (UTC) 26/04 to 054:00 (UTC) 27/04– are also plotted (Fig.5c). ~~The blue dots indicate data points for the first 4 hours in 26/04, while red and orange dots indicate later 4 hours in the morning of 27/04.~~ Since the inaccuracy of modelled BrO is getting larger at lower elevation angles, much attention should be

paid on the large elevation angles. From Fig.5b, we can see obviously that the measured BrO DSCDs before midnight are in good consistence with model for layer 0-1 km. BrO layer between 0-1 km can be considered as the most possible distribution ~~of BrO layer, which is compatible with the measurements~~. Thereby, BrO ~~SCDs can be converted to~~ volume mixing ratios (VMR) are calculated assuming a homogeneous BrO layer of 1 km thickness at the surface.

2.3 Complementary data

Ny-Ålesund is a science community hosting over fifteen permanent research stations. Atmospheric measurements have been measured continuously at Zeppelin Station, Ny-Ålesund since 1990. Located on Zeppelin Mountain with altitude 474 meters a.s.l., it is a background atmosphere observatory operated by NPI (Norwegian Polar Institute) and NILU (Norwegian Institute for Air Research) , which are part of the Global Atmosphere Watch (GAW) Framework.

In Zeppelin Station, ~~S~~surface ozone was measured by UV photometry~~.~~ and ~~G~~gaseous mercury in air was measured using Tekran mercury detector. Hourly Surface Ozone and gaseous mercury data are downloaded at EBAS database (Tørseth et al., 2012).

Meteorology data including temperature, air pressure, relative humidity, wind direction and velocity, and global radiation are recorded by AWIPEV Atmospheric Observatory in Ny-Ålesund. According to the sondes records of temperature, humidity and wind speed from AWIPEV, the height of the troposphere is around 8000 meters and the height of boundary layer is around 1200 meters at Ny-Ålesund.

Webcam on the 474m Zeppelin Mountain records the sea ice change of Kings Bay and the cloud situation of Ny-Ålesund. (https://data.npolar.no/_file/zeppelin/camera/)

In order to get a rough idea of BrO distribution, BrO maps of northern hemisphere by GOME-2 product are downloaded from http://www.iup.uni-bremen.de/doas/scia_data_browser.htm. Stations overpass BrO vertical column densities for MetOp-A (GOME-2A) and MetOp-B (GOME-2B) in Ny-Ålesund, Arctic are downloaded from https://avdc.gsfc.nasa.gov/index.php?site=580525926&id=97.

Using Hybrid Single-Particle Lagrangian Integrated Trajectory (HYSPLIT) model via the NASA ARL READY website (http://www.ready.noaa.gov/ready/open/hysplit4.html) (Draxler and Rolph, 2013;Stein et al., 2015), back trajectory analyses were carried out to find the history of air masses. 72-hours ensemble back trajectories were driven by meteorological fields from the NCEP

带格式的：字
带格式的：字
自动设置
带格式的：字
带格式的：字
New Roman，
动设置
域代码已更改
带格式的：字
自动设置
带格式的：默
带格式的：字
带格式的：字
域代码已更改
带格式的：默
域代码已更改

Global Data Assimilation System (GDAS) model output.

3 Results

Time series of BrO DSCDs at 2°, surface ozone concentrations, solar zenith angle (SZA), air pressure, air temperature, relative humidity, wind velocity and wind direction from 25th April to 15th May are presented in Fig.6. Starting from late afternoon in 26 April, BrO DSCDs clearly exceeded the background levels and peaked at 5.6×10^{14} molecular cm^{-2}. At the same period, surface ozone sharply decreased from ~80 ppb to several ppb and not recovered to normal value until 29 April. During this period, the wind velocity ~~is more than~~changed frequently between 1-7~~5~~ m/s with unstable wind directions and mixing height~~and decreases in 29 April~~. Over a period of one week, elevated BrO levels went back to the detection limit in 4th May under a stable boundary layer. During 4th-5th May, partial ozone (not to near zero level) was depleted in the absence of BrO.

Time series of BrO ~~d~~DSCDs from 14:00 (UTC) 26th April to 12:00 (UTC) 28th April in every elevation angle (2°, 3°, 4°, 6°, 8°, 10°, 15°, 30°) are plotted in Fig. 7. Results of different elevation angles distinguished obviously during the BrO enhancement period. But the differences of the BrO dSCDs ≤4°are very small (upright plot in Fig.7), indicating that the highest value of BrO is probably not above the surface. In order to have a better understanding of the vertical distribution of reactive bromine at Arctic boundary layer, comparison between the measured BrO DSCDs from MAX-DOAS measurements with the modeled ones from SCIATRAN model are performed (Fig.5). Good correlations are found between modeled BrO DSCDs for layer 0-1km and the measured ones during the enhancement. Thereby, ~~BrO layer height between~~ 0-1 km is considered as the most possible distribution of BrO layer~~, which is compatible with the measurements~~. ~~BrO dSCDs distributed from 0-1 km to more likely at 0.5-1 km along with time. This could be explained by that Br/BrO photochemistry reactions are taking place from the boundary layer to the free troposphere where there is enough ozone to react.~~

Sunshine duration, ~~global radiation,~~ SZA, BrO DSCDs from MAX-DOAS at 2° elevation angle, BrO volume mixing ratio, surface ozone and gaseous mercury from 26th-28th April are plotted in Fig. 8. The BrO VMRs were calculated assuming a 0-1 km layer of BrO profile. The highest BrO

带格式的：上
带格式的：上
带格式的：上
带格式的：上
带格式的：上
带格式的：上
带格式的：上
带格式的：字
自动设置
带格式的：字
New Roman，
动设置
带格式的：字
带格式的：字
带格式的：字
带格式的：字

VMR is about 15 pptv during the ODE. Ozone as well as gaseous mercury dropped extremely fast right after the enhancement of BrO. But there seems not sufficient reactive bromine presented locally in the boundary layer since the ozone turned to slowly increase just four hours later (at 231:00 UTC, 26th, April). Afterwards, both ozone and mercury has a slowly recovery with a fluctuation in ~~the~~ 27th Apr~~, afternoon~~. A tiny BrO rise occurred around 20:00 (UTC) on 27th April. This could be explained by that Br/BrO photochemistry reactions are taking place r where there is enough ozone to react. When ozone dropped to the lower limit of the reaction, the reaction of Br+O3→BrO+O2 would stop (the situation at 26th night). When ozone recovered to a certain level, the reaction started again.

带格式的：字
带格式的：字
带格式的：字
带格式的：字
带格式的：非
带格式的：字
带格式的：字
自动设置，图

4 Discussions

In this research, high concentration of troposphere BrO has been detected using the ground-based MAX-DOAS technique. As high as 5.6×10^{14} molecular cm^{-2} BrO column has been detected above Kings Bay, Ny-Ålesund. The retrieval shows that the enhancement occurred accompanied with severe ozone depletion and mercury deposition.

Possible sources of reactive bromine are newly formed sea ice and frost flowers which can provide highly concentrated saline surfaces, thereby adequate ~~sea salt~~bromine aerosols. ~~Another important source is the~~ tTransport of the air masses which already contain elevated BrO or precursors and depleted ozone is another possibility of enhanced BrO. Therefore, we investigate the history of the air masses arriving at measurement site using backward trajectories. Furthermore, the sea ice distribution ~~(Fig.2)~~ and the satellite BrO maps (Fig.10) are important instructions as well.

This enhancement event is a good opportunity to investigate the source of BrO and the impact on the environment of Arctic boundary layer. The following parts are discussed in detail from air mass history, sea ice distribution, and ozone loss and mercury deposition.

4.1 History of air masses

~~Possible sources of reactive bromine are newly formed sea ice and frost flowers which can~~

~~provide highly concentrated saline surfaces, thereby adequate sea salt aerosols. Another important source is the transport of the air masses which already contain elevated BrO and depleted ozone. Therefore, we investigate the history of the air masses arriving at measurement site using backward trajectories. Furthermore, the sea ice distribution (Fig.2) and the satellite BrO maps (Fig.10) are important instructions as well.~~

In order to find the detail of the air mass origin, 72-hour backward trajectories at ~~Ny-Ålesund (~~ 10 and~~,~~ 500~~, 1000~~ meters a.s.l. altitude~~)~~ ~~from 26 April (0600 UTC) to~~ ending at 18:00 (UTC) 27th April ~~(1800 UTC)~~ were calculated every 6 hours (Fig.9a). It shows that air masses at both altitude have a discontinue origin. Then we calculated the air mass backward trajectory ending at 18:00 (UTC) 26th April in every hour (Fig.9a). It shows air mass has different origin before/after 15:00 UTC 26th Apr. The wind direction changed to north with higher velocity. After then, the air mass has a relatively stable origin from 1000 m height. ~~From the map of three altitudes, air masses turned from northwest direction, which is origin from North America to the middle of Arctic Sea. From the vertical distribution of air masses, before noon of 26 April, the air masses came from low boundary layer, while after 18:00 26 April, from the upper troposphere.~~ More trajectory calculations from 22nd April to 30th April are shown in the Appendix Fig. A1 and A2 to take the comparisons.

From the GOME-2 BrO VCD maps from 24th April to 27th April (Fig.10), we can find enhanced BrO are observed at east of Greenland (Red box), far north of Siberia (Blue circle) and east of Spitsbergen (Black box) during the period of interest and the days before. More days BrO Maps from 20 April to 13 May 2015 are shown in the Appendix Fig.A3.

~~GOME-2 BrO VCD maps from GOME-2 measurements from 20 April to 13 May 2015 are shown in Fig. 10. BrO clouds existed at two main periods: coastal North America and Chukchi Sea during 22-23 April and North of Siberia during 08-11 May 2015. Both of the BrO clouds lasted about three to four days, the first of which was occasionally at the same period with the Ny-Ålesund BrO enhancement event.~~ Combining the GOME-2 BrO maps and the trajectory calculations, the ~~role of long range transport~~ source of air masses can be discussed in detail. Firstly, trajectory calculations show that transport from the east coast of Greenland and east coast of Spitsbergen is not possible. So transport from these areas of enhanced BrO can very probably be ruled out. Secondly, trajectories also show that after 16:00 UTC 26 Apr transport from the north

带格式的：字
自动设置
带格式的：上
带格式的：字
自动设置
带格式的：字
带格式的：字
自动设置
带格式的：字
带格式的：字
自动设置
带格式的：字
自动设置，上
带格式的：字
自动设置
带格式的：字
带格式的：字
自动设置
带格式的：字
上标
带格式的：字
自动设置
带格式的：上
带格式的：上
带格式的：字
自动设置
带格式的：缩
符，行距：1.
带格式的：上
带格式的：上
带格式的：字
自动设置
带格式的：字
带格式的：字
带格式的：字
自动设置
带格式的：字
带格式的：字
带格式的：字
带格式的：字
自动设置
带格式的：字
带格式的：字
带格式的：字
自动设置

takes place, which means the high BrO in the blue circle might have influenced this event. However, we have to notice that a). the altitude of air mass is up to 1000 meters; b). there is no enhancement along the path; c). the time scale is unreasonable. The BrO enhancement we found by ground-based MAX-DOAS as well as ozone loss just lasted for several hours. But the high level of BrO in the blue circle area lasted more than one day. ~~Secondly, transport from the north takes place. However, rather low BrO VCDs is showed directly north of Spitsbergen. during the period of interest and the days before, enhanced BrO VCDs are observed northeast of Spitsbergen However, what we found by ground-based MAX-DOAS just lasted for several hours, which is at different time scale. Thereby, air masses transported from high latitude of Arctic from 22 April might have an impact on BrO enhancement in Ny-Ålesund, but not the most critical reason.~~ Additionally, the transport air masses might be the reason of the slowly back BrO_x concentrations to normal values until 3rd May.

带格式的：字
自动设置
带格式的：字
带格式的：字
自动设置
带格式的：默
五号
带格式的：上
带格式的：默
五号

4.2 Sea ice distribution

According to the observation of sea ice concentration from AMSR-E and Zeppelin webcam, Kings Bay is ice-free water area during the measurement period. However, large amount of sea ice appeared at Kings Bay on 26th April (Fig.11), floating from the bay entrance by both wind and tidal forces, which is an unusual phenomenon in the fjord, ~~and lasted for few hours~~. The shape of sea ice was broken ice pieces with irregular border. The ice–sea water mixture was filled in the gaps, which was salty-enriched. From the shape of ice in Fig. 11, the sea ice is not looked like newly formed sea ice because of crashed pieces and corrugated edge. So we consider that the sea ice was formed before floating in the bay and transformed to the ice-water mixture when it came across sharply dropped temperature.

带格式的：缩
行距：1.5 倍
带格式的：上
带格式的：字
自动设置
带格式的：字
带格式的：字
自动设置

The efficient ozone loss is consistent with the temperature decline (Fig.12). The meteorology data shows that on 26th April air temperature continually goes down and reaches bottom of -11.4°C at 22:00. According to the precipitation curve of calcium carbonate, more than 80% of carbonate precipitates below 265K. This process will provide acid aerosol from alkaline sea water, which triggers the transformation of inert sea-salt bromide to reactive bromine (Sander et al., 2006). ~~Although the sun radiation intensity is not strong at that time, the heterogeneous reactions can still~~

带格式的：上
域代码已更改

~~happen under the twilight.~~

It is also worth paying attention that the time period that the sea ice existed and the time BrO started to enhance as well as ozone depleted was not exactly the same. From Fig.8 and 12, the ozone loss started from 14:00 UTC 26th Apr. And as described upon, the sea ice existed in the fjord after 20:00 UTC 26th Apr. It makes the synchronizing variation of BrO and ozone as well as the distribution of 0-1 km reasonable.

Thereby, this BrO enhancement event is more likely a local process, mainly influenced by underlying surface change and local environment. The sea ice is not totally fresh ice but the low air and water temperature in the fjord might cause the formation of brine ice mixture, which is rich in sea salt aerosols. The surface ozone concentrations increased along with the melting of sea ice, which indicated that the life span of BrO radicals are very short. When sea ice disappeared, the reaction immediately ended and reactive bromine radicals gradually transformed to soluble bromide (e.g. HOBr), which explained the sink of it (Fan and Jacob, 1992).

4.3 Kinetic analysis

What makes this case very special is that the increasing rate of BrO and the depletion rate of boundary layer ozone are really fast. The surface ozone reduced by 85% within 4 hours. The ozone loss rate is as high as 10.3 ppbv h^{-1} or 248 ppbv d^{-1}, which is extremely high compared with previous studies in Polar Regions (Tab. 2). The deposition of gaseous mercury occurred concurrently with tropospheric ozone depletion, as well as the enhancement of BrO (Fig. 14), which indicated that the oxidation of GEM by reactive halogen species (Br atoms and BrO radicals) is considered to be the key process of mercury depletion. The GEM decreases from ~2 ng m^{-3} to lower than 0.3 ng m^{-3} during the BrO enhancement event. The mercury loss rate is about ~0.25 ng m^{-3} h^{-1} or 6 ng m^{-3} d^{-1}. The oxidized GEM may directly deposit to snow/ice or associate with particles in the air that can subsequently deposit onto the snow and ice surfaces, and thereby threaten polar ecosystems and human health.

The chemical kinetics of bromine enhancement and ozone decay are analyzed assuming that the catalytic reactions are dominated by reactions showed in Fig.1. A first-order loss of ozone is due to reaction $Br+O_3 \rightarrow BrO+O_2$ resulting in the rate law:

带格式的：字
自动设置

带格式的：正
厘米，行距：

带格式的：字
自动设置

域代码已更改

带格式的：字
文（宋体），（

$$r = -\frac{d[O_3]}{dt} = k_1 \cdot [O_3] \quad \text{(Eq. 1)}$$

$$[O_3] = [O_3]_0 \cdot \exp(-k_1 \cdot t) \quad \text{(Eq. 2)}$$

$$\ln\frac{[O_3]}{[O_3]_0} = -k_1 \cdot t \quad \text{(Eq. 3)}$$

$[O_3]_0$ is the ozone concentration at the beginning of decay determined from the measured mixing ratio of 74.72 ppbv. $\ln\frac{[O_3]}{[O_3]_0}$ versus time are showed as hollow square in Fig. 13a.

According to the method by Jacobi et al. (Jacobi et al., 2006), the first order rate constant k_1 can be determined as follows:

$$\frac{d(\ln\frac{[O_3]}{[O_3]_0})}{dt} = -k_1 \quad \text{(Eq. 4)}$$

The measured decrease of $\ln\frac{[O_3]}{[O_3]_0}$ versus time was fitted by:

$$\ln\frac{[O_3]}{[O_3]_0} = -\exp(b \cdot t + a) \quad \text{(Eq. 5)}$$

$$\frac{d(\ln\frac{[O_3]}{[O_3]_0})}{dt} = -b \cdot \exp(b \cdot t + a) \quad \text{(Eq. 6)}$$

$$\ln(-\ln\frac{[O_3]}{[O_3]_0}) = b \cdot t + a \quad \text{(Eq. 7)}$$

$$k_1 = b \cdot \exp(b \cdot t + a) \quad \text{(Eq. 8)}$$

$\ln(-\ln\frac{[O_3]}{[O_3]_0})$ versus time are plotted as black dots in Fig. 13a. The coefficients a and b are obtained from the linear fit in plot.

The ozone loss begins relatively slow and accelerates with time, which is consistent with the process of bromine explosion.

Assuming that the first order decay is dominated by the reaction $Br+O_3 \rightarrow BrO+O_2$, we are able to calculate the Br concentrations as follows:

$$k_1 = k_{Br} \cdot [Br] \quad \text{(Eq. 9)}$$

$$k_{Br} = 1.7 \cdot 10^{-11} \cdot \exp\left(-\frac{800}{T}\right) \quad \text{(Eq. 10)}$$

k_{Br} is a constant depending on temperature (Fig. 13b). Thereby, the calculated Br concentration increases from 1.1×10^7 to about 1.2×10^9 atoms cm^{-3} (corresponding to 44.8 pptv) (Fig. 13c). Considering the assumption that the halogens are homogenously distributed in the PBL, the concentrations of Br at sea surface layer in the bromine explosion could be even higher.

5 Conclusions

Typical process of enhanced bromine and depleted ozone in Ny-Ålesund boundary layer was observed using ground based MAX-DOAS techniques in late April, 2015. As high as 5.6×10^{14} molecular cm^{-2} BrO DSCDs were detected on 26-27 April. Meanwhile, severe ozone depletion and mercury deposition occurred under BrO VMR of 15 pptv. The model showed enhanced BrO distributed at 0-1 km above the sea surface. By analyzing the air mass history and sea ice conditions, this BrO enhancement event is more likely a local process. The underlying sea ice and low temperature provide acid aerosols, which are prerequisites for the formation of BrO radicals. The kinetic analysis shows that the ozone loss begins relatively slow and accelerates with time, which is consistent with the process of bromine explosion. The ozone loss rate is as high as 10.3 ppbv h^{-1}, which is much higher than previous studies in Polar Regions. GEM loss rate is about ~0.25 ng m^{-3} h^{-1}. This study is a pivotal complement for BrO research in Arctic BL. Further observations and analysis are required to identify the chemical mechanisms.

Acknowledgements.

This research was financially supported by the National Natural Science Foundation of China Project No. 41676184, 41306199 and U1407135. We gratefully thank the Chinese Antarctic and Arctic Administration and the teammates of 2015 Chinese Arctic Expedition. We are also grateful to Dr. Ping Wang from KNMI and Dr. Yang Wang from MPIC for providing the advice on BrO VMR calculation. We kindly acknowledge the AWIPEV Atmospheric Observatory in Ny-Ålesund, the Norwegian Polar Institute and Norwegian Institute for Air Research (NILU) for the complementary data. Caroline Fayt,

Thomas Danckaert and Michel van Roozendael from BIRA are gratefully acknowledged for providing the QDOAS analysis software. Meteorological data, surface ozone, and gaseous mercury were provided by EBAS database. ~~Back trajectories were calculated using the HYSPLIT model from NOAA together with the GDAS data set from NCEP.~~ The authors gratefully acknowledge the NOAA Air Resources Laboratory (ARL) for the provision of the HYSPLIT transport model and READY website (http://www.ready.noaa.gov) used in this publication.

References

Ariya, P. A., Alexei Khalizov, A., and Gidas, A.: Reactions of gaseous mercury with atomic and molecular halogens: Kinetics, product studies, and atmospheric implications, Journal of Physical Chemistry A, 106, 7310-7320, 2002.

Ariya, P. A., Dastoor, A. P., Marc, A., Schroeder, W. H., Leonard, B., Kurt, A., Farhad, R., Andrew, R., Didier, D., and Janick, L.: The arctic: A sink for mercury, Tellus, 56, 397-403, 2004.

Bogumil, K., Orphal, J., Homann, T., Voigt, S., Spietz, P., Fleischmann, O. C., Vogel, A., Hartmann, M., Kromminga, H., and Bovensmann, H.: Measurements of molecular absorption spectra with the sciamachy pre-flight model: Instrument characterization and reference data for atmospheric remote-sensing in the 230~~–2~~380 nm region, Journal of Photochemistry & Photobiology A Chemistry, 157, 167-184, 2003.

Bottenheim, J. W., Netcheva, S., Morin, S., and Nghiem, S. V.: Ozone in the boundary layer air over the arctic ocean: Measurements during the tara transpolar drift 2006-2008, Atmospheric Chemistry & Physics, 9, 4545-4557, 2009.

Chance, K. V., and Spurr, R. J. D.: Ring effect studies: Rayleigh scattering, including molecular parameters for rotational raman scattering, and the fraunhofer spectrum, Applied Optics, 36, 5224-5230, 1997.

Hysplit (hybrid single-particle lagrangian integrated trajectory) model access via ~~noaa~~ NOAA ARL~~arl~~ READY ~~ready~~, 2013.

Fan, S. M., and Jacob, D. J.: Surface ozone depletion in arctic spring sustained by bromine reactions on aerosols, Nature, 359, 522-524, 1992.

Frieß, U., Hollwedel, J., König-Langlo, G., Wagner, T., and Platt, U.: Dynamics and chemistry of

tropospheric bromine explosion events in the antarctic coastal region, Comptes Rendus Des Séances De La Société De Biologie Et De Ses Filiales, 109, 1454-1456, 2004.

Frieß, U., Sihler, H., Sander, R., Pöhler, D., Yilmaz, S., and Platt, U.: The vertical distribution of bro and aerosols in the arctic: Measurements by active and passive differential optical absorption spectroscopy, Journal of Geophysical Research Atmospheres, 116, 597-616, 2011.

Hönninger, G., and Platt, U.: Observations of ~~bro~~ BrO and its vertical distribution during surface ozone depletion at ~~alert~~Alert, Atmospheric Environment, 36, 2481-2489, 2002.

Hebestreit, K., Stutz, J., Rosen, D., Matveiv, V. V., Peleg, M., Luria, M., and Platt, U.: ~~Doas~~ DOAS measurements of tropospheric bromine oxide in mid-latitudes, Science, 283, 55-57, 1999.

Hermans, C., Vandaele, A. C., Fally, S., Carleer, M., Colin, R., Coquart, B., Jenouvrier, A., and Merienne, M. F.: Absorption cross-section of the collision-induced bands of oxygen from the ~~uv~~ UV to the ~~nir~~NIR, Springer Netherlands, 193-202 pp., 2003.

Jacobi, H., Kaleschke, L., Richter, A., Rozanov, A., and Burrows, J. P.: Observation of a fast ozone loss in the marginal ice zone of the Arctic Ocean, Journal of Geophysical Research Atmospheres, 111, 3363-3375, 2006.

Kaleschke, L., Richter, A., Burrows, J., Afe, O., Heygster, G., Notholt, J., Rankin, A. M., Roscoe, H. K., Hollwedel, J., and Wagner, T.: Frost flowers on sea ice as a source of sea salt and their influence on tropospheric halogen chemistry, Geophysical Research Letters, 31, 371-375, 2004.

Kromminga, H., Orphal, J., Spietz, P., Voigt, S., and Burrows, J. P.: New measurements of oclo absorption cross-sections in the 325-435 nm region and their temperature dependence between 213 and 293 k, Journal of Photochemistry & Photobiology A Chemistry, 157, 149-160, 2003.

Kurucz, R. L., Furenlid, I., Brault, J., and Testerman, L.: Solar flux atlas from 296 to 1300 nm, National Solar Observatory Atlas, Sunspot, New Mexico: National Solar Observatory, 1988.

Lehrer, E., Hönninger, G., and Platt, U.: A one dimensional model study of the mechanism of halogen liberation and vertical transport in the polar troposphere, Atmospheric Chemistry & Physics, 4, 2427-2440, 10.5194/acp-4-2427-2004, 2004.

Leser, H., Hönninger, G., and Platt, U.: MaxDOAS measurements of BrO and NO2 in the marine boundary layer, Geophysical Research Letters, 30, 149-164, 2003.

Lindberg, S. E., Brooks, S., Lin, C. J., Scott, K. J., Landis, M. S., Stevens, R. K., Goodsite, M., and Richter, A.: Dynamic oxidation of gaseous mercury in the ~~arctic~~ Arctic troposphere at polar sunrise,

Environmental Science & Technology, 36, 1245-1256, 10.1021/es0111941, 2002.

Lu, J. Y., Schroeder, W. H., Barrie, L. A., Steffen, A., Welch, H. E., Martin, K., Lockhart, L., Hunt, R. V., Boila, G., and Richter, A.: Magnification of atmospheric mercury deposition to polar regions in springtime: The link to tropospheric ozone depletion chemistry, Geophysical Research Letters, 28, 3219-3222, 2001.

Mcconnell, J. C., Henderson, G. S., Barrie, L., Bottenheim, J., Niki, H., Langford, C. H., and Templeton, E. M. J.: Photochemical bromine production implicated in ~~arctic~~ Arctic boundary-layer ozone depletion, Nature, 355, 150-152, 1992.

Neuman, J. A., Nowak, J. B., Huey, L. G., Burkholder, J. B., Dibb, J. E., Holloway, J. S., Liao, J., Peischl, J., Roberts, J. M., and Ryerson, T. B.: Bromine measurements in ozone depleted air over the ~~arctic~~ Arctic ocean, Atmospheric Chemistry & Physics, 10, 6503-6514, 2010.

Pöhler, D., Stephan, G., Zielcke, J., Shepson, P. B., Sihler, H., Stirm, B. H., Frieß, U., Pratt, K. A., Walsh, S., and Simpson, W. R.: Horizontal and vertical distribution of bromine monoxide in northern ~~alaska~~ Alaska during BROMEX~~bromex~~ derived from airborne imaging-doas measurements, EGU General Assembly Conference, 2013.

Platt, U.: Differential optical absorption spectroscopy (DOAS), in: Air monitoring by spectroscopic techniques, m.W. Sigrist, ed, Chem.anal.ser, 32, 327-333, 1994.

Platt, U., and Wagner, T.: Satellite mapping of enhanced bro concentrations in the troposphere, Nature, 395, 486-490, 1998.

Platt, U., and Hönninger, G.: The role of halogen species in the troposphere, Chemosphere, 52, 325, 2003.

Richter, A., Wittrock, F., Eisinger, M., and Burrows, J. P.: Gome observations of tropospheric bro in northern hemispheric spring and summer 1997, Geophysical Research Letters, 25, 2683-2686, 1998.

Rozanov, A., Rozanov, V., Buchwitz, M., Kokhanovsky, A., and Burrows, J. P.: Sciatran 2.0 - A new radiative transfer model for geophysical applications in the 175-2400nm spectral region, Advances in Space Research, 36, 1015-1019, 2005.

Saiz-Lopez, A., Mahajan, A. S., Salmon, R. A., Bauguitte, S. J., Jones, A. E., Roscoe, H. K., and Plane, J. M.: Boundary layer halogens in coastal antarctica, Science, 317, 348-351, 2007.

Saiz-Lopez, A., and von Glasow, R.: Reactive halogen chemistry in the troposphere, Chemical Society Reviews, 41, 6448-6472, 10.1039/c2cs35208g, 2012.

Sander, R., Burrows, J., and Kaleschke, L.: Carbonate precipitation in brine ~~–~~: a potential trigger for tropospheric ozone depletion events, Atmospheric Chemistry & Physics, 6, 4653-4658, 2006.

Schroeder, W. H., Anlauf, K. G., Barrie, L. A., Lu, J. Y., Steffen, A., Schneeberger, Amp, D. R., and Berg, T.: Arctic springtime depletion of mercury, Nature, 394, 331-332, 1998.

Sihler, H., Platt, U., Frieß, U., Doerner, S., and Wagner, T.: Satellite observation of the seasonal distribution of tropospheric bromine monoxide in the arctic and its relation to sea-ice, temperature, and meteorology, EGU General Assembly 2013.

Simpson, W. R., Carlson, D., Nninger, G. H., Douglas, T. A., Sturm, M., Perovich, D., and Platt, U.: First-year sea-ice contact predicts bromine monoxide (BrO) levels at barrow, Alaska better than potential frost flower contact, Atmospheric Chemistry & Physics, 6, 11051-11066, 2007a.

Simpson, W. R., Glasow, R. V., Riedel, K., Anderson, P., Ariya, P., Bottenheim, J., Burrows, J., Carpenter, L. J., Frieß, U., and Goodsite, M. E.: Halogens and their role in polar boundary-layer ozone depletion, Atmospheric Chemistry & Physics, 7, 4375-4418, 2007b.

Sinreich, R., Merten, A., Molina, L., and Volkamer, R.: Parameterizing radiative transfer to convert max-doas dscds into near-surface box averaged mixing ratios and vertical profiles, Atmospheric Measurement Techniques, 5, 7641-7673, 2013.

Steffen, A., Douglas, T., Amyot, M., Ariya, P., Aspmo, K., Berg, T., Bottenheim, J., Brooks, S., Cobbett, F., and Dastoor, A.: A synthesis of atmospheric mercury depletion event chemistry in the atmosphere and snow, Atmospheric Chemistry & Physics, 8, 1445-1482, 2008.

Stein, A. F., Draxler, R. R., Rolph, G. D., Stunder, B. J. B., Cohen, M. D., and Ngan, F.: NOAA's HYSPLIT ~~Noaa's hysplit~~ atmospheric transport and dispersion modeling system, Bulletin of the American Meteorological Society, 96, ~~150504130527006~~2059-2077, 2015.

Stutz, J., Thomas, J. L., Hurlock, S. C., Schneider, M., Glasow, R. V., Piot, M., Gorham, K., Burkhart, J. F., Ziemba, L., and Dibb, J. E.: Longpath doas observations of surface bro at summit, greenland, Atmospheric Chemistry & Physics, 11, 9899-9910, 2011.

Tørseth, K., Aas, W., Breivik, K., Fjæraa, A. M., Fiebig, M., Hjellbrekke, A. G., Lund Myhre, C., Solberg, S., and Yttri, K. E.: Introduction to the european monitoring and evaluation programme (emep) and observed atmospheric composition change during 1972–2009, Atmos. Chem. Phys., 12, 5447-5481, 10.5194/acp-12-5447-2012, 2012.

Tuckermann, M., Ackermann, R., Gölz, C., Lorenzen-Schmidt, H., Senne, T., Stutz, J., Trost, B., Unold,

W., and Platt, U.: Doas observation of halogen radical atalysed arctic boundary layer ozone destruction during the arctoc ampaigns 1995 and 1996 in ny- lesund, spitsbergen, Tellus Series B-chemical & Physical Meteorology, 49, 533-555, 1997.

Vandaele, A. C., Hermans, C., Simon, P. C., Carleer, M., Colins, R., Fally, S., Merienne, M. F., Jenouvrier, A., and Coquart, B.: Measurements of the no2 absorption cross section from 42000cm-1 to 10000cm-1 (238-1000nm) at 220k and 294k, J.~~quant~~Quant.~~spectrosc~~Spectrosc.~~radiat~~Radiat.~~transfer~~Transfer, 59, 171-184, 1998.

Wagner, T., Leue, C., Wenig, M., Pfeilsticker, K., and Platt, U.: Spatial and temporal distribution of enhanced boundary layer bro concentrations measured by the ~~gome~~ Gome instrument aboard ~~ers~~ERS-2, Journal of Geophysical Research Atmospheres, 106235, 225-224, 2001.

Wagner, T., Ibrahim, O., Sinreich, R., Frie, U., Glasow, R. V., and Platt, U.: Enhanced tropospheric bro over ~~antarctic~~ Antarctic sea ice in mid-winter observed by ~~max~~MAX-DOAS ~~doas~~ on board the research vessel ~~polarstern~~Polarstern, Atmospheric Chemistry & Physics, 7, 3129-3142, 2007.

Wilmouth, D. M., Hanisco, T. F., And, N. M. D., and Anderson, J. G.: Fourier transform ultraviolet spectroscopy of the A $^2\Pi_{3/2} \leftarrow X\ ^2\Pi_{3/2}$ Transition of BrO, ~~a 2e aF., And, N. M. D., and Anderson~~Journal of Physical Chemistry A.~~phys.chem.a~~, 103, 8935-8945, 1999.

带格式的: 默
(默认) Times
字体颜色: 自

Table 1. Comparisons of BrO mixing ratio at four main Arctic observation sites

Sites	Observation periods	BrO mixing ratio	Methods	References
Greenland ice sheet (72N, 38W, 3200ma.s.l.)	14 May-15 June 2007, 9 June-8 July 2008	3-5ppt	LP-DOAS	(Stutz et al., 2011)
Barrow, Alaska (71°19'N, 156°40'W)	26 February-16 April 2009	~30ppt	MAX-DOAS LP-DOAS	(Frieß et al., 2011)
Alert, Nunavut (82°32'N, 62°43'W)	20 April- 9 May 2000	~30ppt	MAX-DOAS	(Hönninger and Platt, 2002)
Ny-Ålesund, Svalbard (78.9N, 11.8E)	20 April-27 April 1996	~30ppt	LP-DOAS	(Tuckermann et al., 1997)

Table 2. Comparisons of BrO mixing ratio and ozone loss rate

Method	BrO mixing ratio	Typ. Rate of O3 destruction	References
Observation at PBL	up to 30 pptv	1-2 ppbv h-1	(Tuckermann et al., 1997;Hönninger and Platt, 2002)
Observation at MIZ	~63 pptv	6.7 ppbv h-1 or 160 ppbv d-1	(Jacobi et al., 2006)
Observation at salt lakes	up to 176 pptv	10-20 ppbv h-1	(Hebestreit et al., 1999;Stutz et al., 2011)
Observation at Marine BL	~2 pptv	~0.05 ppbv h-1	(Leser et al., 2003)
Model	30-40 pptv	7.6 ppbv d-1	(Lehrer et al., 2004)
Model	100 pptv	40ppbv d-1	(Fan and Jacob, 1992)
Observation at Ny-Ålesund BL	~15 pptv	10.3 ppbv h^{-1} or 248 ppbv d^{-1}	**this study**

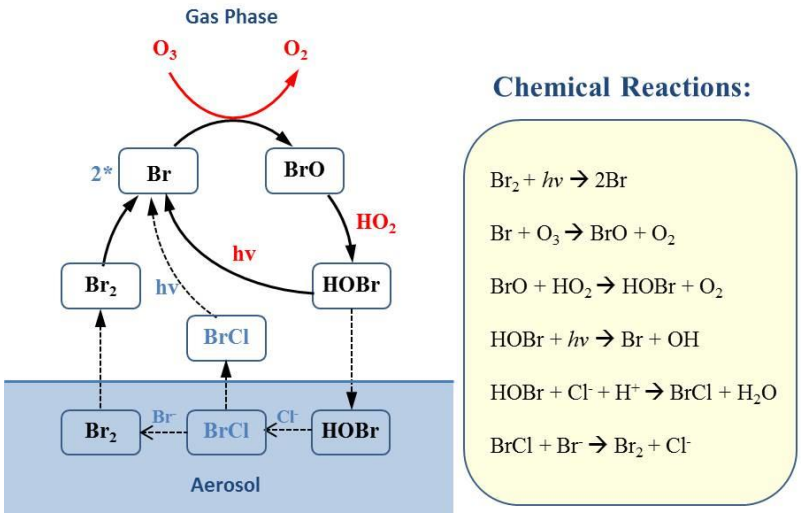

Fig. 1 Chemical reactions of BrO-Ozone cycle

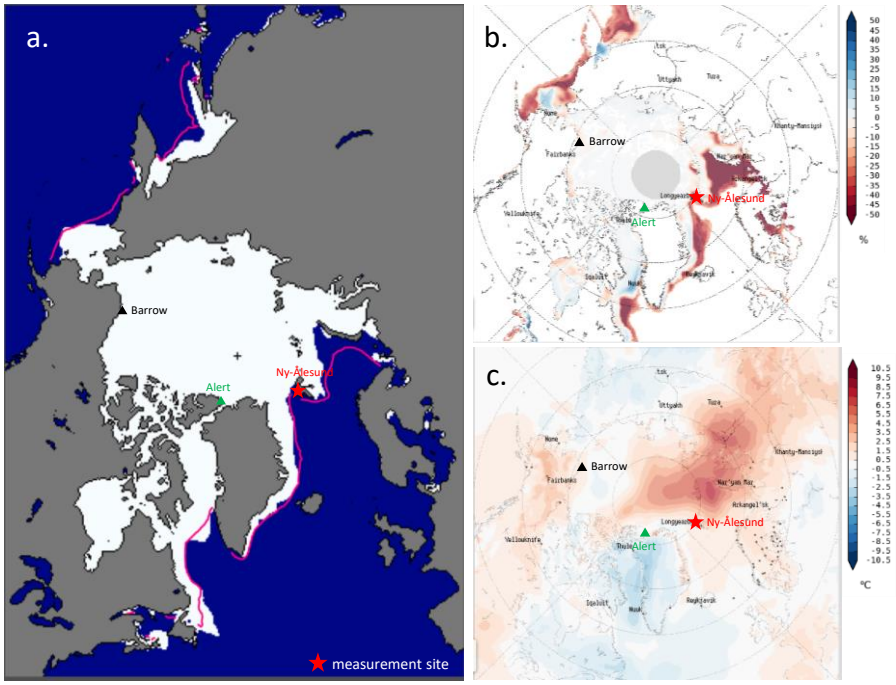

Fig 2. a. Sea ice extent of Apr 2015 in Arctic area (data from http://nsidc.org/data/seaice_index/); b. Monthly mean sea ice concentrations anomalies of April 2015 compare to averages from 1979 to 2015 ; c. Two meters air temperature anomalies of April 2015 compare to averages from 1979 to 2015 (b and c data are from http://nsidc.org/soac)

带格式的：字

带格式的：字

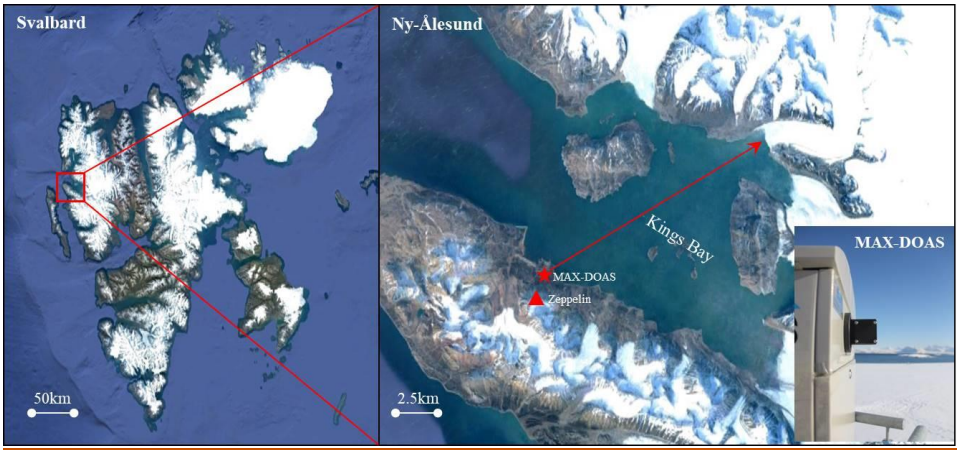

Fig.3 MAX-DOAS field observation in Ny-Ålesund, Arctic

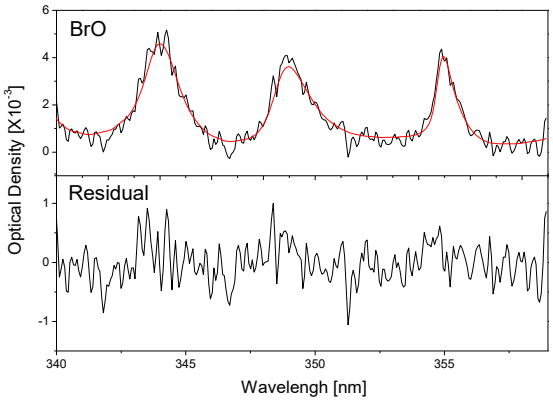

Fig.4 Examples for spectral retrieval of BrO ~~and O4~~. The spectrum was recorded under clear sky conditions at 2 ° elevation on 26 April 2015, 19:59 UTC, SZA = 86 °. (Black lines: Retrieved spectral signatures fitted result for absorber; red lines: fitted cross sections)

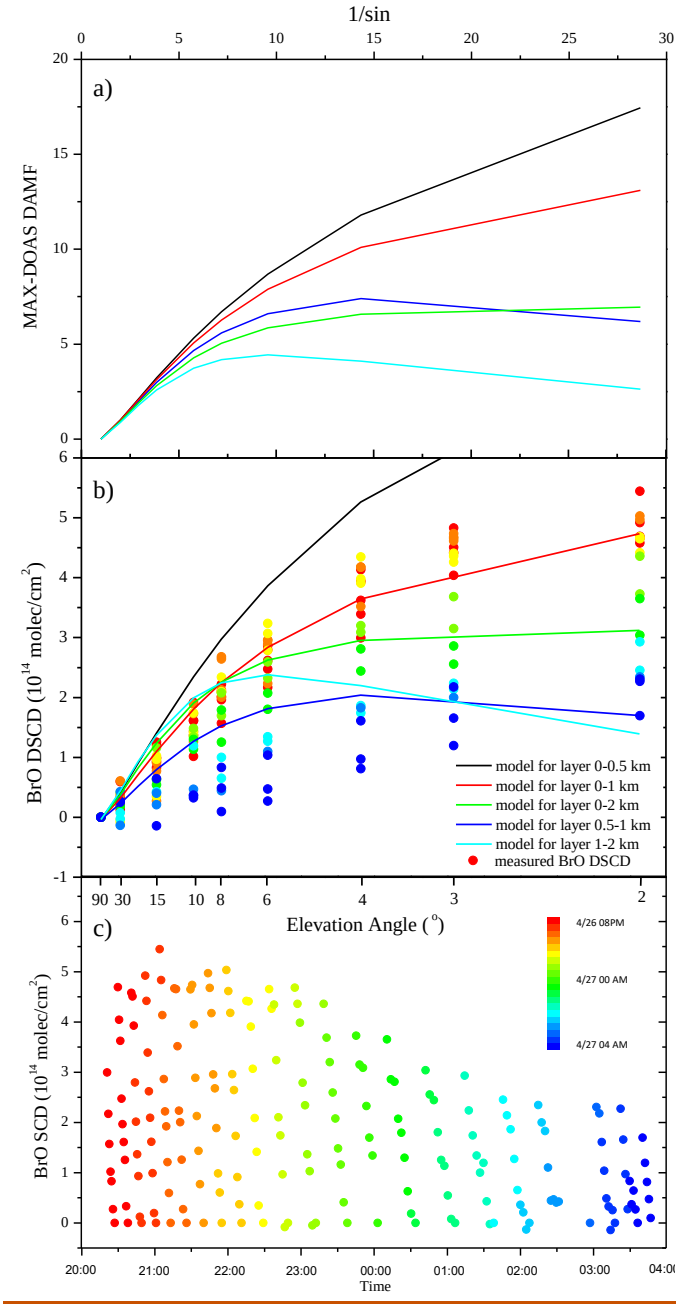

Fig. 5 The modeled DAMF (a) and BrO slant columns (b) using radiative transfer modeling simulation. DAMF are the differences of AMF for low elevation angles and zenith direction. The models are performed assuming a clear sky condition with no aerosol. In part b, the tropospheric BrO VCD is 5×10^{13} molecules/cm^2. The measured BrO DSCDs during the event are also shown (solid dots). The color codes of the measured BrO DSCDs which are also shown in 5b (solid dots) are put into one-to-one correspondence to dots in 5c. ~~The blue dots indicated data points from 20:00 to 24:00 in the evening of 26/04. The red and orange dots indicated data points from 00:00-4:00 in the morning of 27/04.~~

带格式的：字体颜色：自动

带格式的：字体颜色：自动

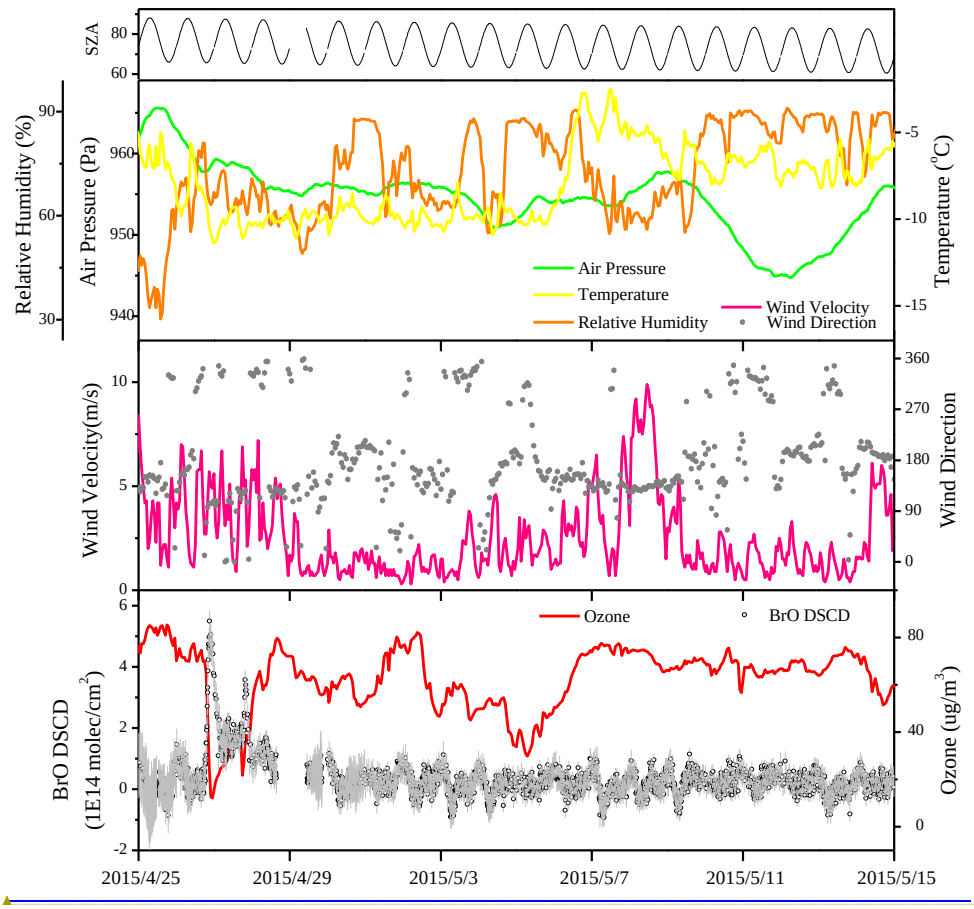

Fig.6 Time series of BrO dSCDs at 2 °, surface ozone, SZA and meteorology data during the measurement.

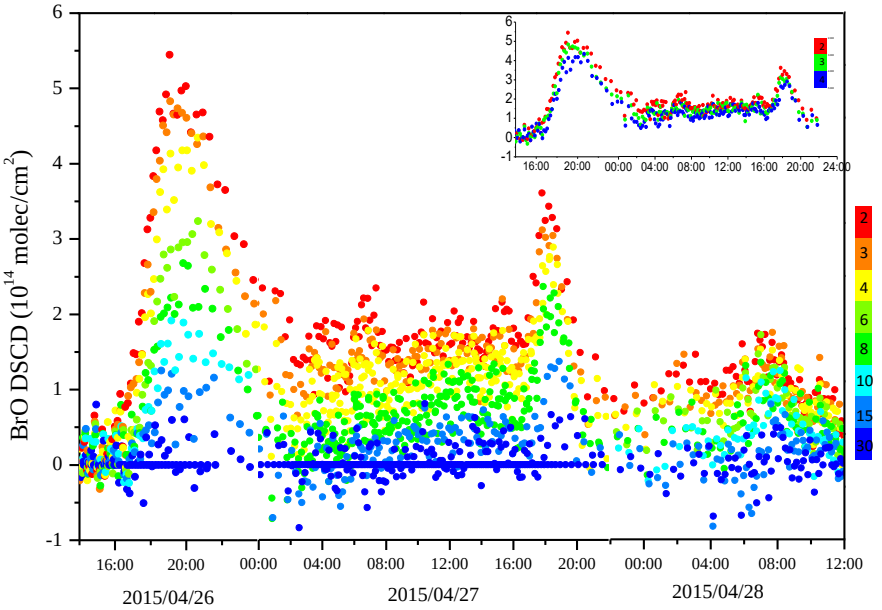

Fig.7 BrO ~~dSCDs~~ DSCDs of different elevation angles during the enhancement period

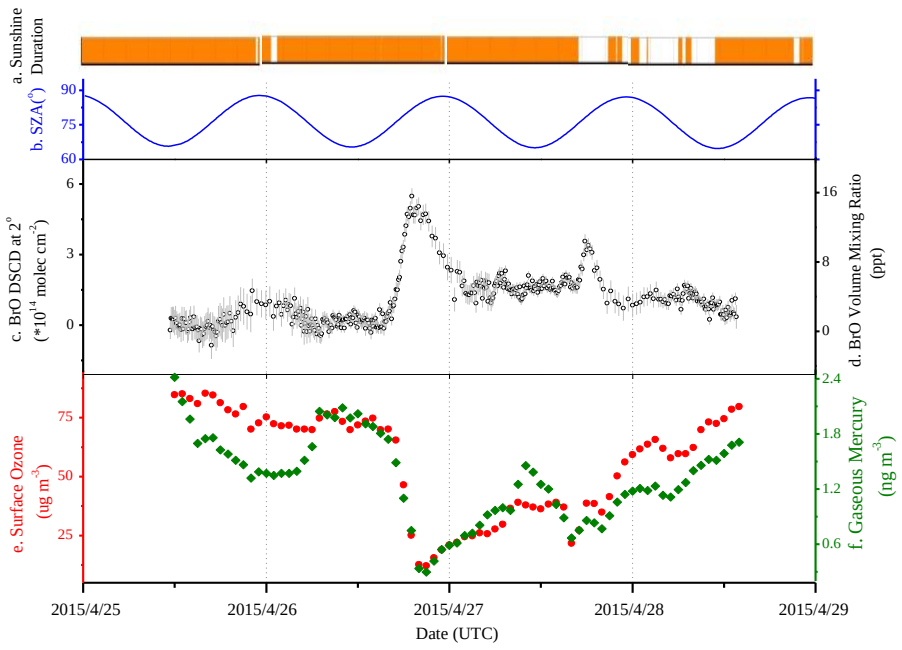

Fig.8 a. ~~Global radiation (W/m^2) (Cited from AWIPEV database)~~Sunshine duration; b. SZA; c. BrO DSCDs from MAX-DOAS at elevation angle 2 °; d. BrO VMR (ppt); e. surface ozone (ug/m^3); and f. gaseous mercury (ng/m^3) from 25/04 noon to 28/04 noon 2015. BrO mixing ratios are calculated assuming a homogeneous BrO layer of 0-1 km.

带格式的：上

带格式的：上

带格式的：上

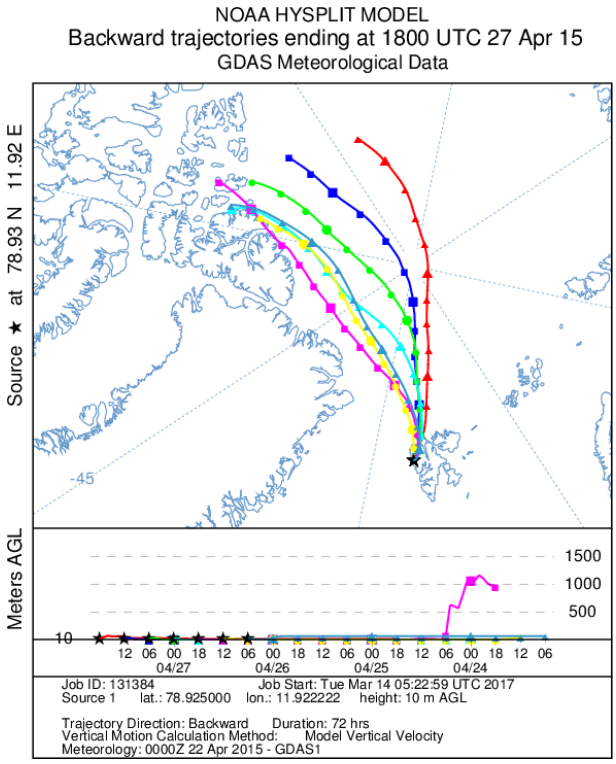

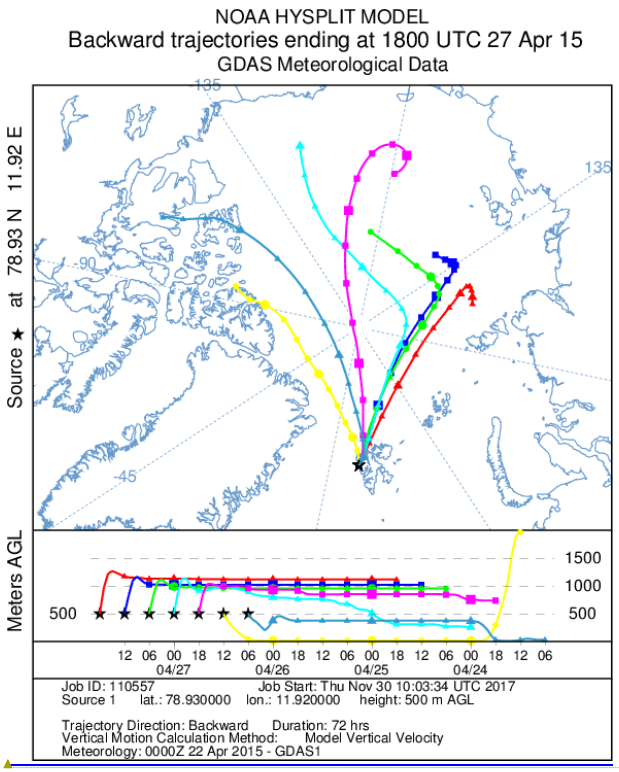

Fig. 9a Back trajectory model of air masses arriving at Ny-Ålesund ~~from 26 April (0600 UTC) to~~ending at 27 April (18:00 UTC) at 10~~,~~ and 500~~, 1000~~ meters a.s.l.. Every 6h a new trajectory starts, each trajectory runs 72h.

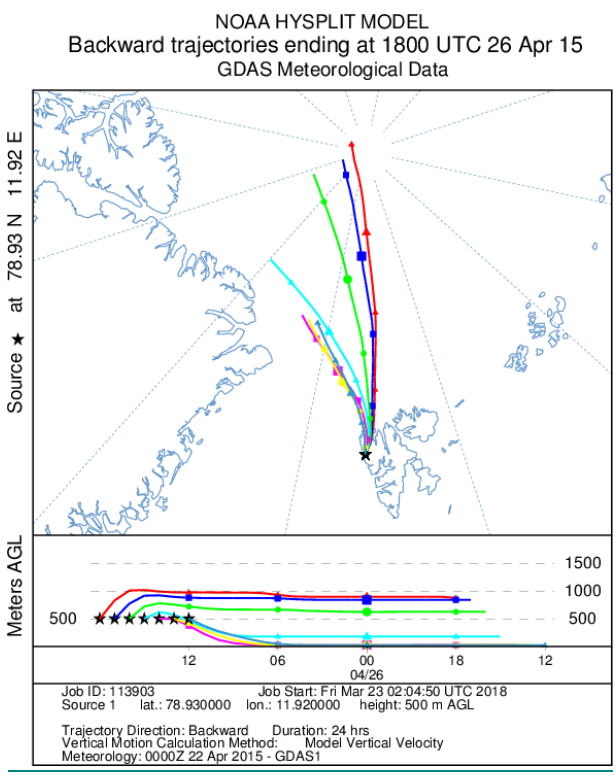

Fig. 9b Back trajectory model of air masses arriving at Ny-Ålesund ending at 26 April (1800 UTC) at 10 and 500 meters a.s.l.. Every 6h a new trajectory starts

带格式的：字
New Roman

带格式的：居

带格式的：左

带格式的：居

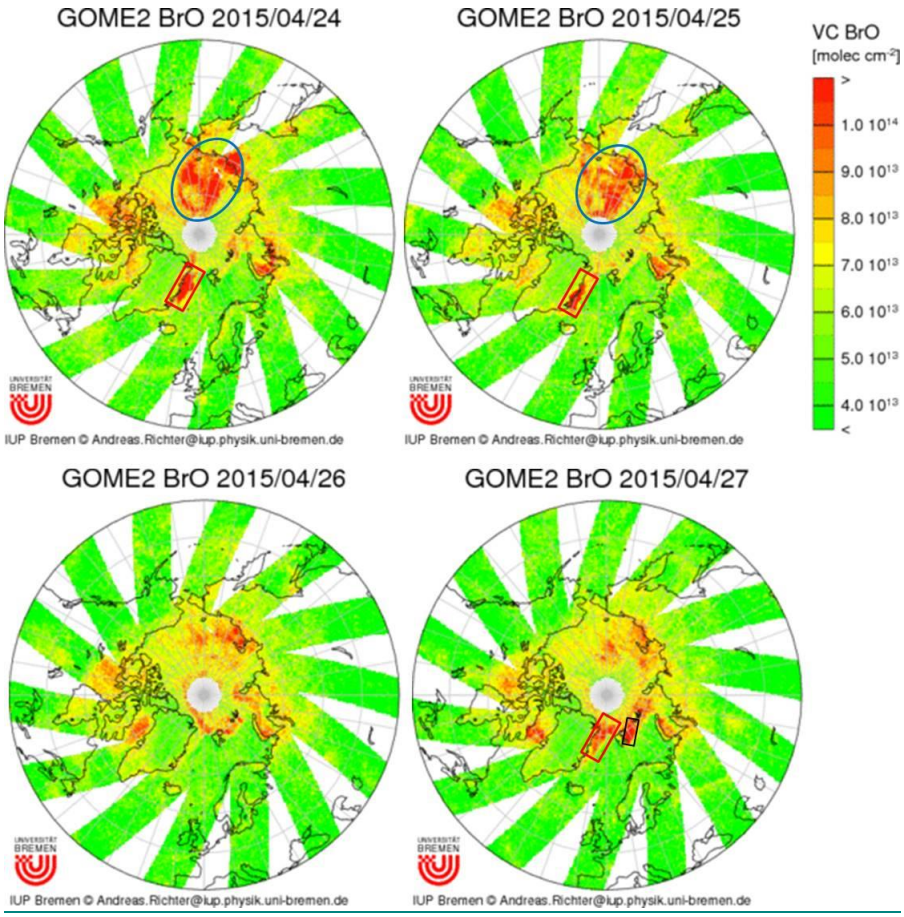

Fig.10 Map of troposphere BrO of northern hemisphere by GOME-2 product from 204 April to 13 27 AprilMay. (Cited from http://www.iup.uni-bremen.de/doas/scia_data_browser.htm)

Fig.11 Sea ice in Kings Bay, Ny-Ålesund at 2221:00 UTC, 26th April 2015

带格式的：上

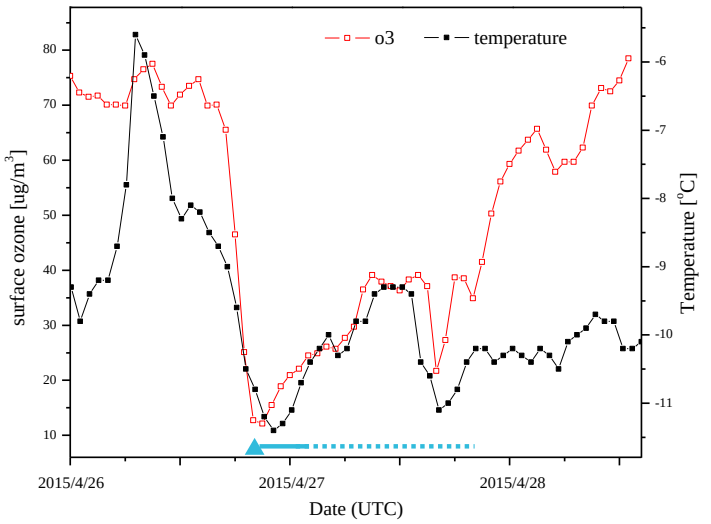

Fig.12 Time series of surface ozone and air temperature during the BrO enhancement event, blue triangles present the sea ice existence in Kings Bay

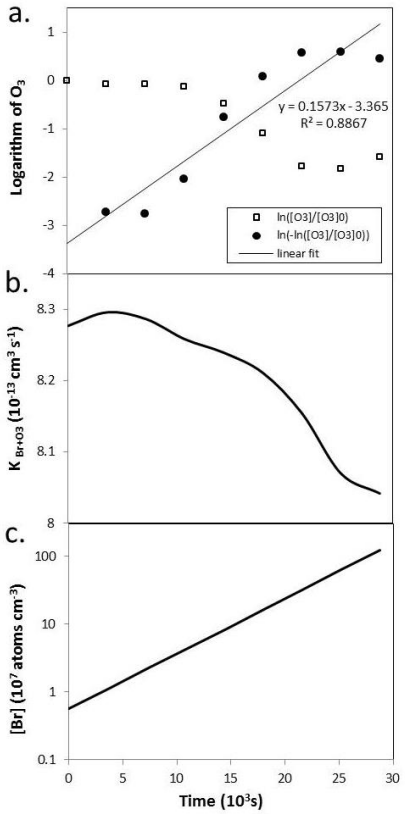

Fig.13 Analysis of surface ozone loss in 26 April 2015

a. Plot of $\ln([O_3]/[O_3]_0)$ and $\ln(-\ln([O_3]/[O_3]_0))$ versus time; b. Calculated temperature dependent reaction rate coefficients for O_3+Br; c. Calculated Br concentration.

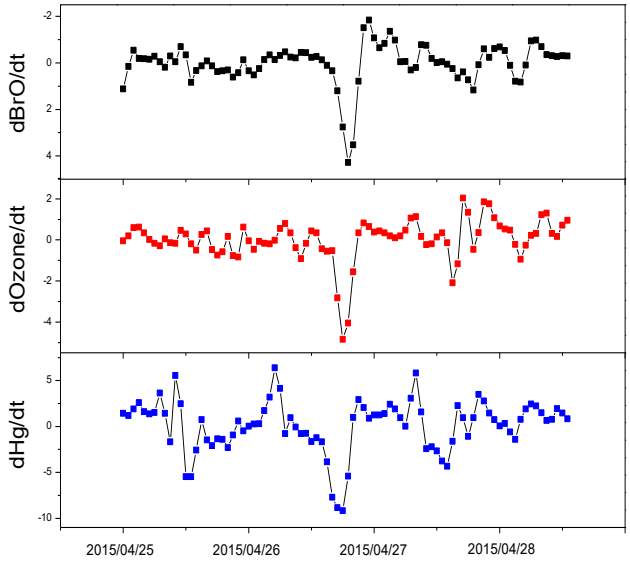

Fig.~~13~~ 14 Time series of dBrO/dt, dO3/dt and dHg/dt during the BrO enhancement event